Reliable Communication Over Rayleigh Fading Channels

by

Ibrahim C. ABOU FAYCAL

Submitted to the Department of Electrical Engineering and Computer Science
in partial fulfillment of the requirements for the degree of

Master of Science
in
Electrical Engineering and Computer Science

at the

MASSACHUSETTS INSTITUTE OF TECHNOLOGY

August, 1996

Author .....
Department of Electrical Engineering and Computer Science
August, 1996

Certified by .....
Mitchell Trott, Assistant Professor
Department of Electrical Engineering and Computer Science
Thesis Supervisor

Accepted by .....
F.R. Morgenthaler
Chair, Departmental Committee on Graduate Students
Department of Electrical Engineering and Computer Science

Reliable Communication Over Rayleigh Fading Channels

by

Ibrahim C. ABOU FAYCAL

Submitted to the Department of Electrical Engineering and Computer Science on August 9, 1996, in partial fulfillment of the requirements for the degree of Master of Science in Electrical Engineering and Computer Science

Abstract

Channels exhibiting fading and dispersion are often used for communication purposes, especially on a wireless medium. Understanding how these channels differ from the ideal Gaussian channel is of great interest. But since the capacity of such channels is difficult and sometimes impossible to obtain, one can always try to characterize the conditions that achieve capacity, provide bounds, or analyze a "good" high performance scheme where high transmission rate and low probability of error are achieved.

Under such a motive, we initially study and summarize a technical report written by John S. Richters for the Research Laboratory of Electronics in November 1967 [1]. This report considers the transmission of digital information over continuous-time fading dispersive channels, subject to a bandwidth constraint on the input signals. A specific signaling scheme is proposed and the problem is modeled as block coding over successive independent uses of a diversity channel. The discrete-time model obtained can be characterized as an *independent identically distributed* Rayleigh fading channel. Lower and upper bounds for the minimum attainable probability of error are derived for this model.

The capacity of the discrete-time IID Rayleigh fading channel is studied next. The capacity achieving distribution is proved to be discrete and having a mass point at zero. Graphs representing capacity and the corresponding optimal distribution are generated numerically, the behavior of the channel at low SNR is studied, and finally a comparison with the ideal additive Gaussian noise channel is drawn.

Thesis Supervisor: Mitchell Trott
Title: Assistant Professor of Electrical Engineering and Computer Science

Acknowledgments

I am greatly indebted to my advisor Professor Mitchell D. Trott for guidance, encouragement and support throughout the course of this study. In addition to having confidence in me, he was very understanding and supportive. Thanks are due to Professor Shlomo Shamai for suggesting this problem and patiently discussing many of its aspects with me. I would like also to thank my officemates at the Laboratory for Information and Decision Systems for numerous helpful discussions and enlightened comments. A fabulous academic and social environment at MIT made my studies at the institute one of the most enjoyable experiences of my life.

I am very grateful to his excellency President Elias Hrawi for his infinite support, advise and parental care, without which the dream of pursuing my studies wouldn't have come true. I am also grateful to Mr. Issam Fares and Fares Foundation for their support and encouragement during my graduate studies, and for making this research possible. Thanks are due also to NSF grant NCR-9314341 for funding the last part of this research.

The list of my friends of the Lebanese Club at MIT is very long. They have made my stay very enjoyable in Boston, and I would like to thank them all.

There are of course no words to describe my gratitude to my parents. They have been always there when I needed them, they believed in me, and made me who I am. I only hope this work will make them proud of their son.

To my parents,

Siham and Chafik

Table of Contents

1 Introduction 11

1.1 Motivation and Background 11

1.2 Outline of the Thesis 12

2 Richters' Report 13

2.1 Introduction 13

2.2 Channel Model 14
Transmission of One Input Signal 15
Transmission of More than One Input Signal 15
Comments 18

2.3 Bounds to Error Probability 19
Expurgated Bound 19
Random-Coding and Sphere-Packing Bounds 26
Capacity 29

2.4 Results and Interpretation 30
Discussion of the Results 30
Application to the Communication Problem 32
Numerical Examples 35

2.5 Summary and Conclusion 35

3 The Capacity of an IID Rayleigh Fading Channel 37

3.1 The Kuhn-Tucker Condition 37

3.2 The Discrete Character of X^* 38
Assuming the Support of X^* Infinite 38
Conclusion 40

3.3 The Existence of an Impulse at Zero 40
The Mutual Information 41
Conclusion 43

3.4 Assumption 43

3.5 Numerical Results 44
The Algorithm 45
The Gradient 45
The Step Size 46
The Projection 46
The Number of Impulses 48

Final Algorithm 51
Results and Analysis 51
Conclusion 57

4 Summary and Conclusions **59**

4.1 Summary 59
4.2 Future Work 60

Appendix A The Kuhn-Tucker Condition 63

Appendix B The Accumulation Point 67

Appendix C Proof of Theorem 1 69

Appendix D Condition for an Additional Impulse 71

Bibliography 73

List of Figures

Figure 2.1: p_1 and p_2 versus a. 22

Figure 2.2: x_o^2 versus a. 22

Figure 2.3: $E_{xe}(\infty, a, 1)$ versus a. 23

Figure 2.4: Optimizing $\{x_n\}$ versus a, K=ρ=1. 24

Figure 2.5: Optimum $\{p_n\}$ versus a, K=ρ=1. 24

Figure 2.6: Optimum r vs. a, K=1. 25

Figure 2.7: $E_{xe}(r, a, 1)$ versus a. 25

Figure 2.8: p_1 and p_2 versus a/K, for $E_{oe}[\infty,a,K]$. 28

Figure 2.9: x_o^2 versus a/K, for $E_{oe}[\infty,a,K]$. 28

Figure 2.10: $C(a,1)/a$ versus a. 30

Figure 2.11: Exponents for Equivalent Gaussian and Fading Channels. 31

Figure 2.12: Capacities for Equivalent Gaussian and Fading Channels. 32

Figure 3.1: The Slope ρ of the Curve $C(a)$ 45

Figure 3.2: Projection on the Simplex in 3D 47

Figure 3.3: Splitting vs. Non-Splitting 50

Figure 3.4: Capacity versus Power 52

Figure 3.5: Optimal Locations versus Power 52

Figure 3.6: Corresponding Optimal Probabilities 53

Figure 3.7: Probability and Location of the Non-Zero Impulse. 55

Figure 3.8: The Fading Channel Compared to the Gaussian Channel. 56

Figure 3.9: The Ratio of Capacities 57

Chapter 1

Introduction

1.1 Motivation and Background

Channels exhibiting fading and dispersion are often used for communication purposes, especially on a wireless medium. Perhaps the best known examples of such channels are radio links. The user is generally interested in reliably transmitting at the highest possible rate. But what is this rate? The capacity of such time-varying channels is difficult and sometimes impossible to obtain, even numerically. As an alternative, one can always try to characterize the conditions that achieve capacity, provide bounds, or analyze a "good" high performance scheme where high rate and low probability of error are achieved. These approaches help obtain a better understanding of the performance limits of such channels, in order to give systems designers a goal to aim at.

In a technical report written for the Research Laboratory of Electronics in November 1967 [1], John S. Richters tried to answer these questions while considering the transmission of digital information over continuous-time fading dispersive channels with a large number of independent scatterers, so that the fading has a Rayleigh-distributed amplitude and a uniform phase. He proposed a specific signaling scheme, and modeled the problem as block coding over successive independent uses of a diversity channel. He derived lower and upper bounds for the minimum attainable probability of error using the expurgated bound, the random coding bound, and the sphere packing bound. In addition, he computed numerically the capacity of the Rayleigh fading channel and compared it to the capacity of an ideal Gaussian channel.

Although Richters' study seems to be important and interesting, it strangely does not appear to be cited in the literature. This could be explained by the unusual nature of his results: the optimal distribution on the input signal levels for the different bounds is found to be discrete, a rather unexpected result on a continuous-time channel. It may also be due

to the difficulty one finds in relating Richters' model to real channels. Many of his assumptions are unrealistic and some appear to be made just in order to obtain a "nice" framework, even when they are far from reality and sometimes absurd. The most striking example is his use of interleaving on a slowly time-varying channel, in order to get back into the framework in which successive symbols face independent and identically distributed (IID) fading. Normally, one would try to estimate the channel on such a medium and then use the estimate instead of throwing out the channel state information. The optimality of few other assumptions made in the report is also in question.

1.2 Outline of the Thesis

The main focus of our work is reliable communication over continuous, IID Rayleigh-fading, dispersive channels. We use Richters' report as our main reference, and we view our study to be complementary to it.

The thesis is divided into two parts. In the first part, we summarize and comment on Richters' report. In the second, we study in depth the capacity of a discrete-time Rayleigh fading channel in which successive symbols face independent fading. We prove first the impulsive nature of the capacity achieving distribution on the input levels, which was missing from the report. Next, we try to locate the mass points of the optimal distribution, and prove specifically that one of them is located at zero. In addition, since the numerical simulation in the original work done by Richters is somewhat primitive, we regenerate some of the results and extend them to more interesting cases, where previously simulation was practically unfeasible. This allows us to verify the results obtained in the original work and ours. Another interesting aspect we investigate is how the optimal input distribution varies as a function of the power constraint. We have also a particular interest in the behavior of this channel at low SNR.

Chapter 2

Richters' Report

As it was mentioned previously, in his study, Richters has obtained some unusual results: the optimal distribution on the input signal levels for the different bounds is found to be discrete, a rather unexpected result on a continuous-time channel.

As a first part of our research, we have tried to understand Richters' report and summarize it in a simple fashion. We have expressed few remarks on his work, and tried to investigate how his study can be improved and extended. Special attention is given to the results obtained for what can be interpreted as an IID Rayleigh fading channel, and how different it is compared to the ideal Gaussian channel.

2.1 Introduction

The main concerns in the report were:

1. To use channels exhibiting both fading and dispersion for digital communication purposes with a bandwidth constrained input signal set.
2. To obtain a greater understanding of the performance limits of such channels.
3. By providing bounds on the performance of such systems, to give systems designers a goal to aim at.

Consider the transmission of one of M equiprobable signals at a rate $R=\ln(M)/T$ nats/sec. Assume the channel is composed of a large number of point scatterers, and characterized by a scattering function $\sigma(r,f)$. The approach adopted, and exposed in the following sections, is to consider a set of N basic signals designed so that each is independently affected by the channel. The problem then reduces to coding over N symbols.

In Section 2.2 the model is derived, in Section 2.3 bounds on the error probability are

determined, and in Section 2.4 the results obtained are exposed, and related to the communication problem.

2.2 Channel Model

The problem under consideration is the transmission of information over a linear, continuous-time, fading, dispersive channel. Any narrow-band input signal $s(t) = Re\{u(t)e^{jw_0 t}\}$ affected by a particular scatterer with range r seconds and shift f Hertz results approximately in the output $o(t) = Re\{Au(t-r)e^{j[(w_0-2\pi f)t - w_o r]}\}$. Since small differences in r can lead to extreme phase differences in the received component, it is reasonable to consider the quantity $\theta = -w_o r$ as a random variable uniformly distributed over $(0,2\pi)$. A large number of independent scatterers with range r and Doppler shift f, each with random phase and approximately the same reflection coefficient, results in an output

$$o(t, r, f) = Re\{A(r, f)e^{j\theta(r,f)}u(t-r)e^{j[(w_0-2\pi f)t]}\}, \tag{2.1}$$

where $A(r,f)$ will tend to have a Rayleigh distribution, while $\theta(r,f)$ will become uniform (i.e., the fading coefficient is a complex circular Gaussian random variable). The *scattering function* of the channel is $\sigma(r,f)=E[A^2(r, f)/2]$. It is assumed that there is *no average energy loss through the channel* (or that such loss is accounted by a normalization of the input signal level). The scattering function $\sigma(r,f)$ may be approximately characterized by two quantities: the Doppler spread B, and the multipath spread L. If $\sigma(r,f)$ is unimodal and well behaved, then the fading of any two waveforms should essentially be independent if they are separated by more than $1/B$ seconds or more than $1/L$ Hertz. If a signal has a duration of T seconds and a bandwidth of W Hertz, the number of independently faded samples in the output process has been shown by Kennedy [4] to be:

$$K = \begin{cases} (1+BT)(1+WL) & \text{if } BL \le 1 \text{ or } TW = 1 \\ (T+L)(W+B) & \text{otherwise.} \end{cases} \tag{2.2}$$

Relation (2.2) will be interpreted later as an approximation to the number of diversity paths available.

2.2.1 Transmission of One Input Signal

Richters studied first the transmission of an input $xs(t)$, where $s(t)$ is a unit-energy signal and where x is the amplitude. Assume that the noise is additive white Gaussian, and thus the output $r(t)$ can be written as the sum of the signal $o(t) = \int_0^\infty \int_0^\infty o(t, r, f)drdf$ (Eq. (2.1)) and a noise term $n(t)$ whose power spectrum is $N_o/2$. If $r(t)$ is expressed in a Karhunen-Loève expansion using the eigenfunctions of the autocorrelation function of $o(t)$, the coefficients r_k corresponding to the eigenvalues λ_k will be complex circular (i.e., having a uniform phase) and uncorrelated. Having the coefficients r_k's complex is due to the fact that the eigenfunctions are complex. If we condition on the input, the assumption of Rayleigh fading and Gaussian noise ensures that the r_k's are jointly Gaussian, and therefore they will form a set of *independent* sufficient statistics.

2.2.2 Transmission of More than One Input Signal

One would like to generalize this procedure to the case where more than one input signal is sent. We would like to obtain a set of basis functions that yield uncorrelated output components for any of the input signals used, while being able at the same time to uniquely separate the input at the output. If one of two input signals is sent, we can use the fact that any two symmetric positive-definite matrices can be simultaneously diagonalized to find a (non-orthogonal) expansion that results in uncorrelated components of $\underline{r}$. However, for M arbitrary signals, such an expansion does not exist. Moreover, and more importantly, if the input signals excite the same output components, they cannot be separated at the output because they will result in crosstalk. If, however, one starts with a carefully chosen set of input signals that has these two properties, then it is possible to consider coding over this signal set and compute some error probabilities.

The Signal Set

Richters chose for this purpose a signal set of N time and frequency translates of one basic unit-energy signal, with sufficient guard spaces allowed so that the output signals are independent and orthogonal. Let T_s be the duration of the basic signal and W_s its bandwidth. Separating the signals in the set by L seconds will make the output signals approximately

orthogonal, and an additional $1/B$ will make them independent. Therefore, let the guard space in time be $T_g=L+1/B$. The same analysis holds for the guard space in frequency which is made $W_g=B+1/L$. Let us construct the M input signals by simultaneously amplitude-modulating the N basic signals, so each input is characterized by a vector $\underline{x}_m$, where x_{mn} is the modulation of the n^{th} basic signal. We require an average power constraint:

$$\frac{1}{M}\cdot\sum_{m=1}^{M}\sum_{n=1}^{N}x_{mn}^2\le TP,$$

where P is the output signal power.

The Probability Distribution Characterizing the Channel

Let's find the probability distribution characterizing the channel: p(output/input). For this purpose, consider first the original problem with the one basic input signal $xs(t)$. Given the input x, the k^{th} component of $\underline{r}$ is a zero-mean circular complex Gaussian random variable, with variance $(x^2\lambda_k+N_o)/2$, and thus, it is only necessary to record its squared amplitude $y_k=r_{k,re}{}^2+r_{k,im}{}^2$ (since there is no information in the phase). Normalized by N_o, y_k has a central chi-square distribution $p_{\lambda_k}(y_k/x)$ with two degrees of freedom, which is exactly an exponential distribution with "parameter" $1/(1+x^2\lambda_k/N_o)$.

Without loss of generality, we replace x^2/N_o with x^2 and absorb N_o into the energy constraint:

$$\frac{1}{M}\cdot\sum_{m=1}^{M}\sum_{n=1}^{N}x_{mn}^2\le\frac{TP}{N_o}.$$

The vector $\underline{y}$ of components y_k is a set of sufficient statistics which, given x, has a density being a product of exponentials. We will denote its density by $p_{\underline{\lambda}}(\underline{y}/x)$, where the vector $\underline{\lambda}$ is given by $\underline{\lambda}=[\lambda_1,\ \dots\ ,\ \lambda_K]$.

Since the N basic signals were chosen to yield independent and orthogonal outputs, the previous result can be easily generalized to simultaneous modulation and transmission of each signal, reducing the problem conceptually to N uses of a memoryless continuous-amplitude, discrete-time channel. The guard spaces T_g and W_g between adjacent signals and the signal durations T_s and W_s determine N as

$$N = \frac{TW}{(T_s + T_g)(W_s + W_g)} \qquad \frac{1}{M} \cdot \sum_{n=1}^{N} \sum_{m=1}^{M} x^2_{mn} \le Na ,$$

where $a=(P/N_oW)(T_s+T_g)(W_s+W_g)$. The number of positive λ_k's will be approximated by the previously given K in Eq. (2.2).

Remarks on the Choice of the Signal Set

By allowing each of the basic signals to be different, one can conceivably do better than with the present scheme. However in the model described above, $p_{\underline{\lambda}}(\underline{y}/x)$ is the same for a given input signal wherever it is placed in the time-frequency space, and thus, a basic signal is "good" no matter where it is placed, and Richters conjectures that not much will be gained by allowing the N signals to be different. Note that there is no simple relation between the vector $\underline{\lambda}$ and the input signal $u(t)$, and finding one of them given the other is a very difficult problem, so in the report the analysis was done based on $\underline{\lambda}$, T_s and W_s, with the problem of finding the corresponding $u(t)$ ignored. Moreover, the study will be restricted later to the equal-eigenvalues case, and the problem of finding a "good" basic signal will become finding a good T_s,W_s combination: what is the best number of degrees of freedom for the basic signal to have?

Slowly Time-Varying Channels

One last point that needs to be addressed here is the waste of bandwidth in this scheme when the guard space is too large. Richters uses interleaving to reduce this guard space when B or L are small, in which case there are no orthogonality problems (in other words, the scattering function has a narrow shape, and the channel varies slowly in time and frequency), but large guard space is required to obtain independent output signals. In this case the number of signals increases to $N_{sc}=TW/(T_s+L)(W_s+B)$, and

$$\frac{1}{M} \cdot \sum_{n=1}^{N_{sc}} \sum_{m=1}^{M} x^2_{mn} \le N_{sc} a_{sc} \qquad \text{where} \qquad a_{sc} = \frac{P}{N_o W}(T_s + L)(W_s + B) .$$

In this framework, where no channel identification is attempted, interleaving is clearly uniformly better than the non-interleaving scheme.

A simple and useful case studied in the following sections is the equal-eigenvalues case, $\lambda_k = 1/K \; \forall k \in \{1, \ldots, K\}$, for which the probability distribution of the vector $\underline{y}$ involves only the sum of the components $y = y_1 + \ldots + y_K$, which becomes thus a sufficient statistic, with density

$$p_K(y/x) = \frac{y^{K-1} \exp\left(-\frac{y}{1 + x^2/K}\right)}{\Gamma(K)(1 + x^2/K)^K}. \tag{2.3}$$

In this case, the channel model becomes scalar-input/scalar-output.

2.2.3 Comments

From the equations derived above, we can see that the model may be considered as N independent uses of a classical diversity channel with K equal-strength paths. As it was mentioned earlier, on a slowly time-varying channel, one ought to estimate the channel and use the estimate to improve detection. Richters instead uses interleaving in order to get into the IID framework he has chosen to work in; this unrealistic assumption made his results far from real systems. Among the rare applications that can be modeled this way is a fast frequency hopping system with multiple receiving antennas, for which each symbol is transmitted on a different frequency. In such a system, the fast hopping is used to enhance security at the cost of diminished communication rate.

Note also that a discrete-time IID Rayleigh fading model explicitly *does not* arise from sampling a rapidly time-varying channel at the Nyquist rate of the input process. If the time variations were fast enough to cause independent fading at each symbol, then the bandwidth of the output process would be larger than that of the input process, necessiting oversampling. This can also be seen by recognizing that the channel will vary considerably within a symbol, so that a symbol-rate sampler cannot possibly extract a sufficient statistic.

Another point that merits examination is how far is the assumption of equal-eigenvalues from real systems. As mentioned before, the correspondence between $\underline{\lambda}$ and the input signal is difficult to establish and we only have tried to intuitively understand and relate the model to real systems. We expect that with a basic signal spread over more than one coherence bandwidth or one coherence time of the channel, we will get more than one

non-zero eigenvalue, but it is intuitive also to expect the strength of the different paths to be non equal, with a smooth transition, for example, from one non-zero eigenvalue to two. On the other hand, as the number of non-zero eigenvalues increases, we expect many of them to be of relatively equal strength and the model just derived may be applied.

2.3 Bounds to Error Probability

In this section, we will summarize and expose the various results Richters has obtained for the miscellaneous bounds on the minimum attainable probability of error. In Section 2.3.1 the expurgated upper bound is analyzed and in Section 2.3.2 the random-coding upper bound is studied together with the sphere-packing lower bound.

The central problem considered here is finding the optimum input density and the resulting error probability bound for block coding over N uses of a continuous-amplitude, discrete-time channel model derived in the preceding section. The major result is that the optimum density consists of a finite set of impulses, a rather unexpected result for a continuous channel.

2.3.1 Expurgated Bound

The expurgated bound derived by Gallager for the scalar-input/scalar-output channel, and extended by Yudkin to the vector-output channel, is given by

$$P_e < \exp -N\{E_x[\rho, p(x), r] - \rho[R_N + \Delta_N]\} \qquad \text{where} \quad \lim_{N\to\infty} \Delta_N = 0 \quad \text{and} \quad R_N = \frac{\ln M}{N}$$

$$E_x[\rho, p(x), r] = -\rho \ln\left[\int_0^\infty \left(\int_0^\infty p(x)p(x_1)e^{r(-2a + x^2 + x_1^2)} H_{\underline{\lambda}}(x, x_1)^{1/\rho} dx_1\right) dx\right]$$

$$\text{and } H_{\underline{\lambda}}(x, x_1) = \int_0^\infty p_{\underline{\lambda}}(\underline{y}/x)^{1/2} p_{\underline{\lambda}}(\underline{y}/x_1)^{1/2} d\underline{y} = \prod_{k=1}^{\infty} \frac{(1 + \lambda_k x^2)^{1/2}(1 + \lambda_k x_1^2)^{1/2}}{1 + \frac{1}{2}\lambda_k(x^2 + x_1^2)}$$

$$\rho \geq 1 \qquad r \geq 0 \qquad \int_0^\infty x^2 p(x)dx = a \qquad \text{and} \qquad \sum_{n=1}^{N} x_{mn}^2 \leq Na\,.$$

The difficulty lies in finding the r, $p(x)$ combination that achieves the tightest bound, that

is, maximizes $E_x[\rho, p(x), r]$. For this particular channel model it turns out that no local-minima problems arise. A sufficient condition for r and $p(x)$, given the constraints, is for them to satisfy the equation

$$\int_0^\infty p(x_1) e^{r(x^2+x_1^2)} H_{\underline{\lambda}}(x, x_1)^{1/\rho} dx_1 \geq \int_0^\infty \left(\int_0^\infty p(x) p(x_1) e^{r(x^2+x_1^2)} H_{\underline{\lambda}}(x, x_1)^{1/\rho} dx_1 \right) dx \qquad (2.4)$$

for all $x \geq 0, 0 < \rho < \infty$ with equality when $p(x) > 0$.

The determination of such r and $p(x)$ is a difficult matter, and the adopted solution was to take some particular values, plug them into the equation and see whether equality holds. In order to simplify the analysis and gain insight into the basic factors involved, Richters restricted his study to the equal-eigenvalues case, with K non-zero eigenvalues. Note that the optimum exponent for an arbitrary $\underline{\lambda}$, $E_x(\rho, a, \underline{\lambda})$, can be lower bounded by an equal-eigenvalue exponent E_{xe} (a subscript "e" will be added to the different quantities when the equal-eigenvalues assumption is made).

Before proceeding with the summary of this study, it is worthwhile stopping at the above sufficient condition (2.4) derived by Richters in one of the appendices. On the left hand side of the inequality we have, for a given $p(x)$, a function of x denoted $f(x)$, while on the right hand side we have the weighted average of $f(x)$ on a selected set where $p(x)$ is non-zero. The condition states then that $f(x)$ should be greater than "its weighted average on the support of $p(x)$" for any x, with equality where $p(x)$ is non-zero. If we draw a graph of $f(x)$, since it has to be greater or equal to the right hand side for all x's, we clearly see that the support of $p(x)$ must be a subset of the set where $f(x)$ achieves its minimum. Intuitively it seems hard for a function to have a "flat minimum" so that the support of $p(x)$ can be continuous, and thus we expect that a solution to this inequality will be most likely a discrete density.

Condition (2.4) is thus seen to play an important role in determining the characteristics of the optimal probability density, and a thorough inspection of the correctness of its derivation should be considered. Although we believe that the result is true, we should mention that the derivations appear to be mathematically incorrect: Richters didn't take into account that $p(x)$ is in general a distribution. Instead, he just considered it to be a function.

One last observation that should be mentioned here, is that the report states that it can be proven that the above condition is also a necessary condition for the optimal r and $p(x)$ to satisfy.

Going back to the K equal-eigenvalues problem, it can be easily shown that $E_{xe}(\rho,a,K)$ is equal to $K.E_{xe}(\rho/K,\ a/K,\ 1)$ and thus, as far as the minimization is concerned, K can be set to 1 and the range of ρ extended from zero to infinity.

In another appendix Richters shows that, if a solution for the above problem exists, it is unique. Since the study of the zero-rate exponent ($\rho=\infty$) is simple compared to the general case, it was conducted first.

Zero-Rate Exponent

The optimization problem turns out to be easier in this case, and yet the results indicative of those that will be obtained for positive rates. Note that studying the zero-rate exponent is interesting for many other reasons: this exponent is tight and we will discuss later how. The zero-rate exponent is valid when the number of code words grows less than exponentially with the block length (in a polynomial fashion for example). Therefore, from a practical point of view, this exponent is useful when short blocks are to be used.

When ρ is taken to infinity, the optimal r is found to be zero, and the sufficient condition becomes:

$$\int_0^\infty p(x_1)\ln H_1(x,x_1)dx_1 \geq \int_0^\infty \left(\int_0^\infty p(x)p(x_1)\ln H_1(x,x_1)dx_1\right)dx + \alpha_o(x^2-a)\,,$$

for some α_o, with equality when $p(x) > 0$.

It is shown that a density of the form $p(x)=p_1\delta(x)+p_2\delta(x-x_o)$ satisfies the condition for all a when the parameters are correctly chosen. Therefore, the optimum density consists of two impulses, one of which is at the origin. Note that this result is sharper than what we have derived in Chapter 3 for capacity. In Chapter 3, we are not able to determine for sure whether two impulses are enough for some range of the power constraint; instead, we show the result numerically.

The location x_o of the second impulse and the probabilities p_1, p_2=1-p_1 can be computed and they are shown in Fig. 2.1 and 2.2.

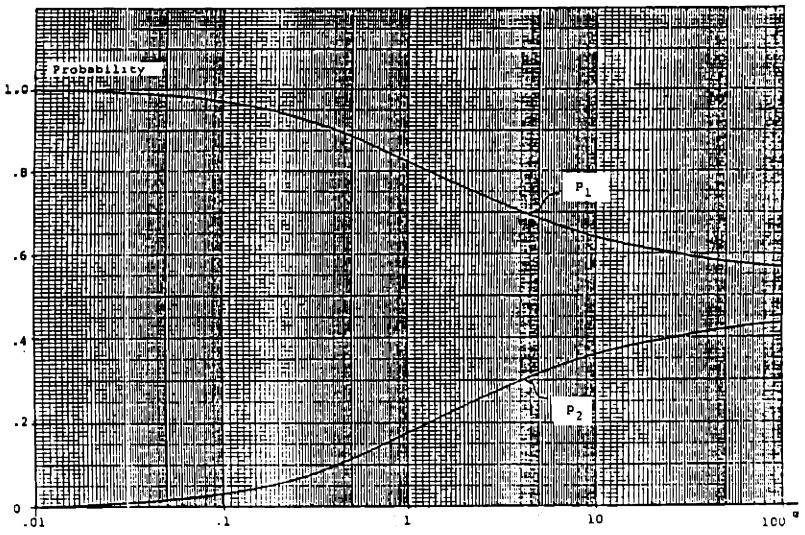

Figure 2.1: *p_1 and p_2 versus a.*

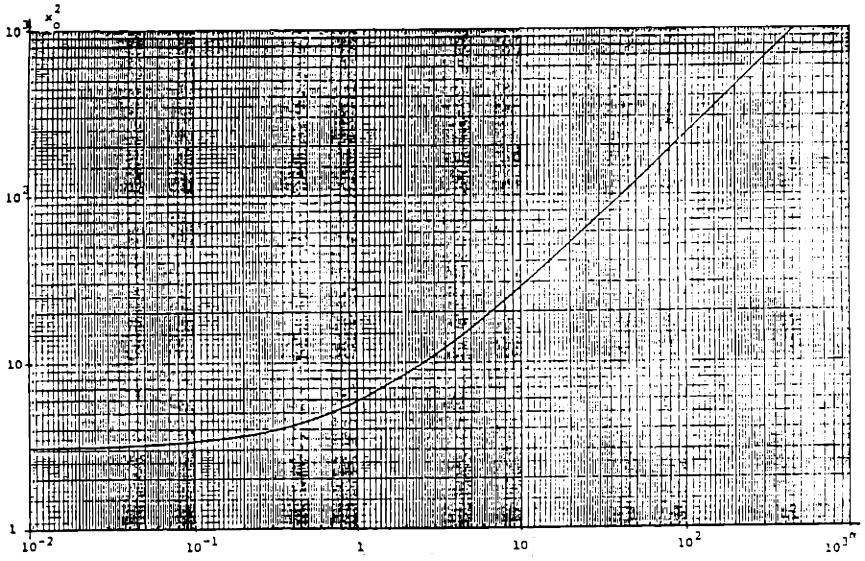

Figure 2.2: *x_o^2 versus a.*

The location x_o of the second impulse seems to have an asymptote as a goes to zero. This behavior is essentially different from what we will obtain in Chapter 3 for capacity: for very low a, we also found that two impulses are to the accuracy of the simulations enough, but x_o goes very slowly to infinity.

On Fig. 2.3 $E_{xe}(\infty, a, 1)$ is drawn versus the power constraint a.

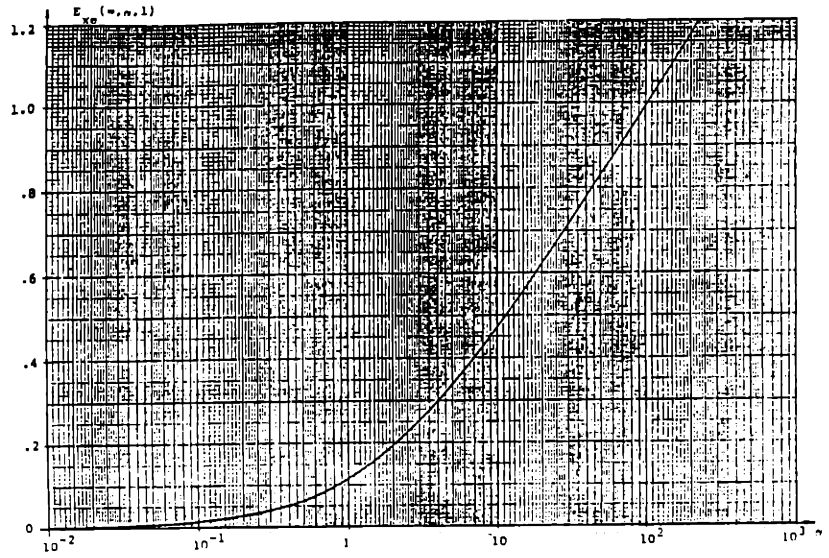

Figure 2.3: $E_{xe}(\infty, a, 1)$ *versus* a.

Positive Rates

The study in Richters' report was restricted to the case where K=1. It is shown in the report that condition (2.4) must be satisfied by some r, $p(x)$ combination, where $0 \leq r \leq 1/2\rho$ and $p(x)$ consists of a finite number of impulses, located at x_n's where $0 \leq x_n^2 \leq z_\rho$, z_ρ being finite and a function of only ρ and a. Even knowing that a finite set of impulses achieves the optimum, the problem was still very hard to solve, except in the special case when a is small. In this case, it is shown that a two-impulse distribution will asymptotically satisfy the sufficient condition, when a goes to zero. Moreover Richters states that it is also possible to show that the two-impulse distribution is optimal for small non-zero a. The proposed proof amounts to specifying values of ρ and a, under the assumption of a two-impulse density, solving for the optimum probabilities, positions, and r, and then numerically verifying that the resulting $p(x)$ does satisfy condition (2.4). One would like very much to obtain an analytical proof of this result as we conjecture that a similar property holds for the achieving capacity distribution studied in Chapter 3. Unfortunately we were not able to derive this result.

In general, for any given value of ρ and a, a numerical solution was computed by first specifying a grid $\{x_n\}$ and then minimizing over $\{p_n\}$ for a range of values of r, because in a joint minimization over $\{x_n\}$, $\{p_n\}$ and r the function to be minimized is not a convex

function. As the grid $\{x_n\}$ gets small, the solution is expected to get very close to the true minimizing $p(x)$ and r. The results obtained are reproduced in Fig. 2.4, 2.5 and 2.6.

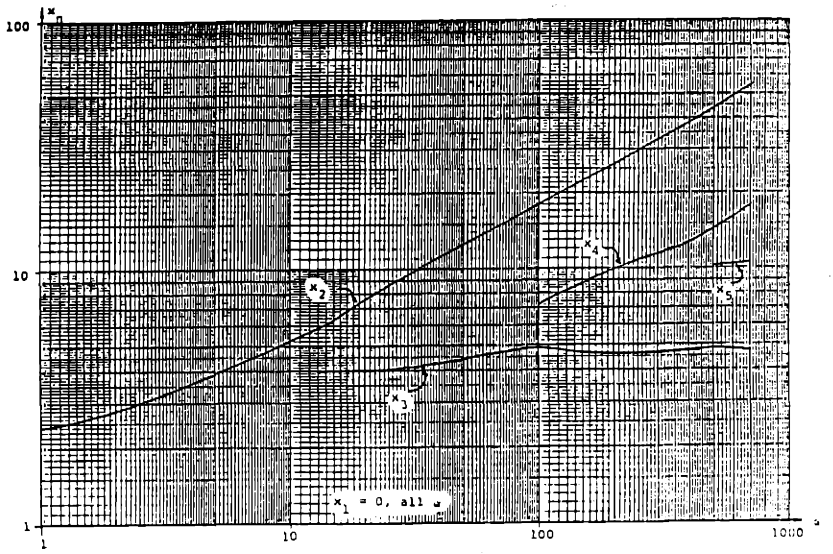

Figure 2.4: *Optimizing* $\{x_n\}$ *versus a,* $K=\rho=1$.

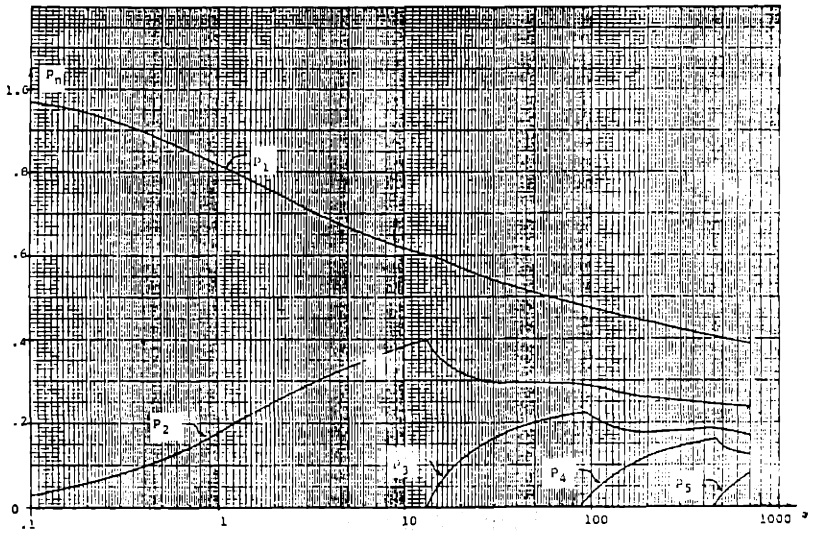

Figure 2.5: *Optimum* $\{p_n\}$ *versus a,* $K=\rho=1$.

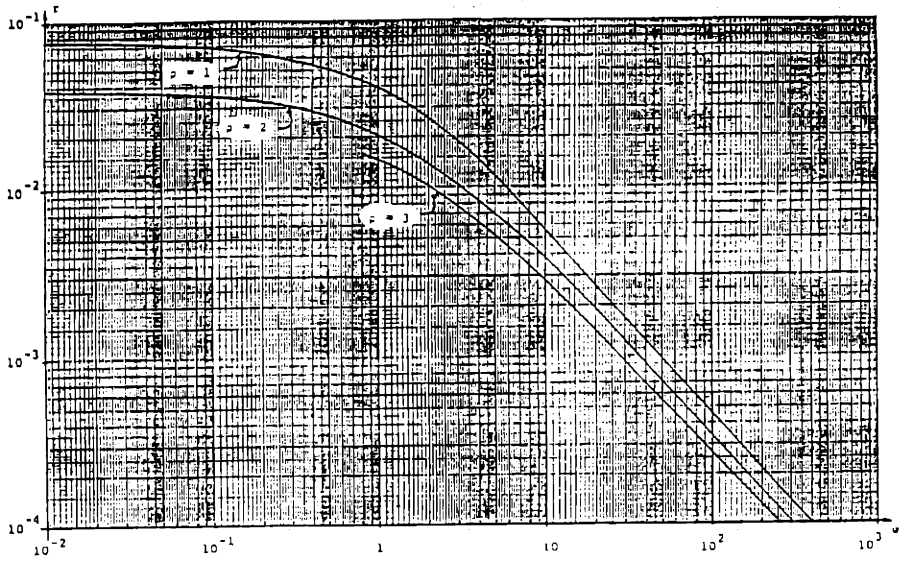

Figure 2.6: *Optimum r vs. a, K*=1.

In Fig. 2.7 E_{xe} was drawn versus a for different values of ρ one of them being ρ=1, a curve of particular interest as it represents the cutoff rate.

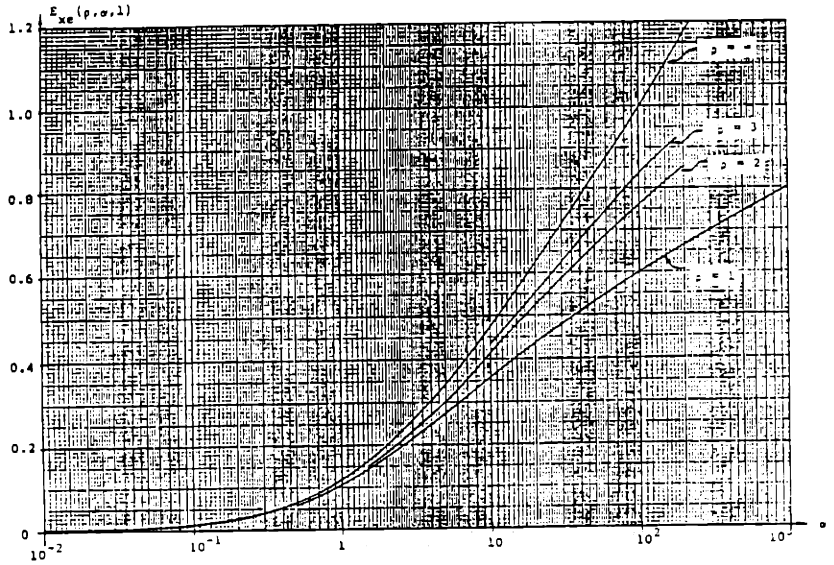

Figure 2.7: $E_{xe}(\rho, a, 1)$ *versus a.*

From the observation of these plots, Richters conjectures the following properties:

1. The optimum density always contains an impulse at the origin, an observation explained by Richters by the fact that zero is the input that results in the smallest variance at the output, and that zero is also "good" for the energy constraint.

2. For any given K and ρ, the solution starts with two impulses when a is near zero, and the number of these impulses increases with a, by steps of 1.

3. For a given value of K and ρ, r decreases with a and appears to have an asymptote.

4. When a new impulse appears, its probability is at the expense of the one that appeared before.

In the zero-rate case ($\rho=\infty$), when a and N were fixed, there was a monotonic improvement in the exponent when K was increased, while this is no longer the case when $\rho<\infty$. We were not able to provide an explanation to this result, as one should expect the opposite to happen: an improvement in the exponent as more diversity is acquired. A possible interpretation of this phenomena is that, by increasing the amount of diversity for a fixed amount of input energy, this energy is split among too many diversity paths, and detection suffers.

2.3.2 Random-Coding and Sphere-Packing Bounds

The random-coding upper bound to error probability as derived by Gallager states that if each code word is constrained to satisfy

$$\sum_{n=1}^{N} x_{mn}^2 \le Na \qquad \text{then, for any } 0 \le s \le \frac{1}{2} \text{ and } r \ge 0$$

$$P_e < \exp -N\left\{E_o\left[\frac{s}{1-s}, p(x), r\right] - \frac{s}{1-s}R_N - \zeta_N\right\} \qquad \text{where } \int_0^\infty x^2 p(x)dx = a \quad \text{and}$$

$$E_o\left[\frac{s}{1-s}, p(x), r\right] = -\ln \int_0^\infty \left[\int_0^\infty p(x) p_{\underline{\lambda}}(\underline{y}/x_1)^{1-s} e^{r(x^2-a)} dx\right]^{1/(1-s)} d\underline{y}\,,$$

where $\zeta_N \to 0$ as $N \to \infty$, and where s is related to the conventional parameter ρ by

$$s = \frac{\rho}{(1+\rho)}\,.$$

Because of the integration over $\underline{y}$, the minimization is complex for arbitrary $\underline{\lambda}$, so Richters' study was restricted to the equal-eigenvalues systems, where $\underline{y}$ reduces to a scalar. One should notice that in the current formulation, it is not possible to remove K from the problem as it was possible for the expurgated bound. A sufficient condition for r and $p(x)$ to be optimum under the above constraints is for them to satisfy

$$\int_0^\infty \beta(y)^{s/(1-s)} p(y/x)^{1-s} e^{rx^2} dx \ge \int_0^\infty \beta(y)^{1/(1-s)} dy \qquad \text{for all x, when } 0 < s < 1\,, \tag{2.5}$$

$$\beta(y) \equiv \int_0^\infty p(x) e^{rx^2} p(y/x)^{1-s} dx\,.$$

In his report, Richters proves that this condition must be satisfied by an r, $p(x)$ combination where $0 \leq r \leq K(1-s)$, and $p(x)$ being a finite set of impulses at locations x_n's found as previously between zero and a function of s, a and K. Equation (2.5) and the impulsive solution are both valid for $0<s<1$ and not only in the (0,1/2] range. This extension was seen necessary for consideration of the lower bound

$$P_e > \exp -N\left[max_{0 \leq s \leq 1}\left\{ E_{oe}\left[\frac{s}{1-s}, a, K\right] - \frac{s}{1-s}(R_N - \Delta_N)\right\} + \delta_N\right].$$

$Eoe[s/(1-s),a,K]$ is E_o evaluated at the minimizing $p(x)$ and r for a given value of a, and for the K equal-eigenvalues case.

Zero-Rate Bound

The zero-rate bound corresponds to the case where $s \rightarrow 1$. The zero-rate sphere-packing bound is probably not useful because, at least for discrete memoryless channels, the *straight-line bound* due to Shannon, Gallager, and Berlekamp (1967) is better. The straight-line lower bound has the same zero-rate exponent as the expurgated upper bound. Therefore, the zero-rate exponent of the expurgated bound is tight for the DMC, and we believe that this result is also true for Richters' channel. Nonetheless Richters' results were the following: r was found to be zero and two impulses are optimum, one of them being located at the origin. Furthermore, in this special case K can be normalized into a as it was done previously. In Fig. 2.8 and 2.9 the probability density coefficients and the location of the non-zero amplitude pulse were drawn versus a/K.

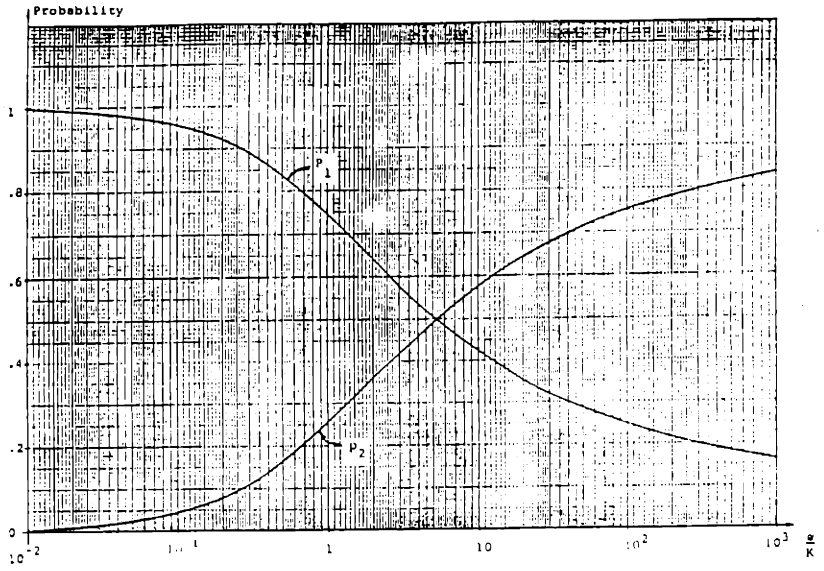

Figure 2.8: p_1 *and* p_2 *versus* $\frac{a}{K}$, *for* $E_{oe}[\infty,a,K]$.

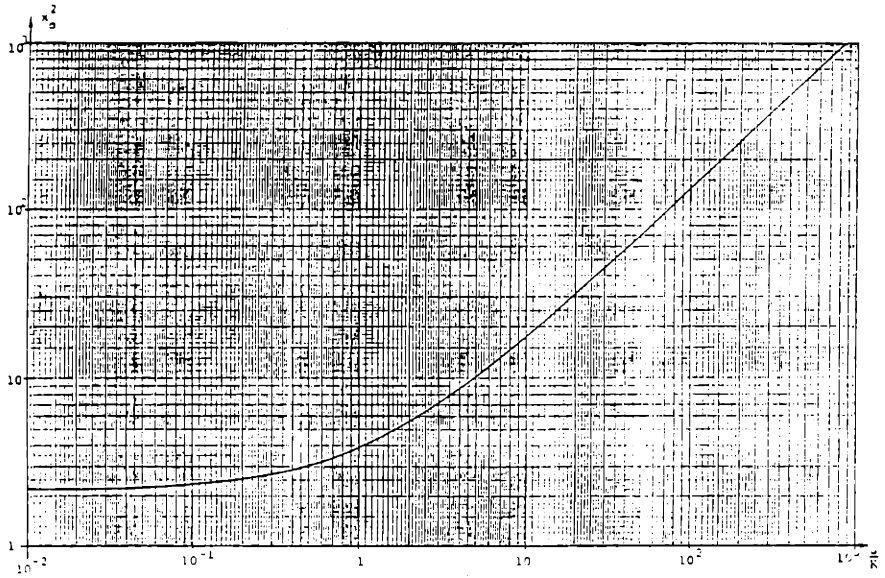

Figure 2.9: x_o^2 *versus* $\frac{a}{K}$, *for* $E_{oe}[\infty,a,K]$.

Positive Rates

The results here were much harder to obtain beyond the fact that an impulsive density is optimum, except for the special case where s=1/2 (or ρ=1) where, as expected, the exponent of the expurgated bound is obtained again. One additional result than can be stated here is that a two-impulse distribution will again asymptotically satisfy the condition as a goes to zero.

2.3.3 Capacity

The capacity of the IID Rayleigh fading channel will be studied in detail in Chapter 3. In this section we will only summarize Richters' results.

By letting $s \to 0$ it is proven that $r=0$ is optimum, and the problem becomes the maximization of the rate. This maximum rate, the capacity of the channel, is

$$C(a, K) = \int_0^\infty \left(\int_0^\infty p(x)p(y/x) \ln \left[\frac{p(y/x)}{\int_0^\infty p(x_1)p(y/x_1)dx_1} \right] dy \right) dx .$$

A sufficient condition on $p(x)$ for the maximization of $C(a,K)$, subject to the constraint is

$$\gamma\left(x^2 - \frac{a}{K}\right) + C(a, K) \geq \int_0^\infty p(y/x) \ln \left[\frac{p(y/x)}{\int_0^\infty p(x_1)p(y/x_1)dx_1} \right] dy$$

$$\text{for all} \quad x \geq 0, \qquad \text{with equality when } p(x) > 0 .$$

We can clearly see that the above condition is exactly the Kuhn-Tucker condition on capacity, where the term on the right hand side is the divergence (or Kullback-Leibler distance) between $p(y/x)$ and $p(y)$, and the first term on the left hand side being just a Lagrange multiplier reflecting the energy constraint.

Once again, when $a \to 0$ Richters finds numerically that two impulses will asymptotically be optimum, and results in the infinite-bandwidth capacity which is the same as for the additive white Gaussian noise channel with the same value of P/N_o.

In Fig. 2.10, $C(a,K)/a$ is plotted versus a. It is unfortunate that the report did not provide a plot of $C(a,K)$ "alone" against a, which might be a more representative plot than the one provided.

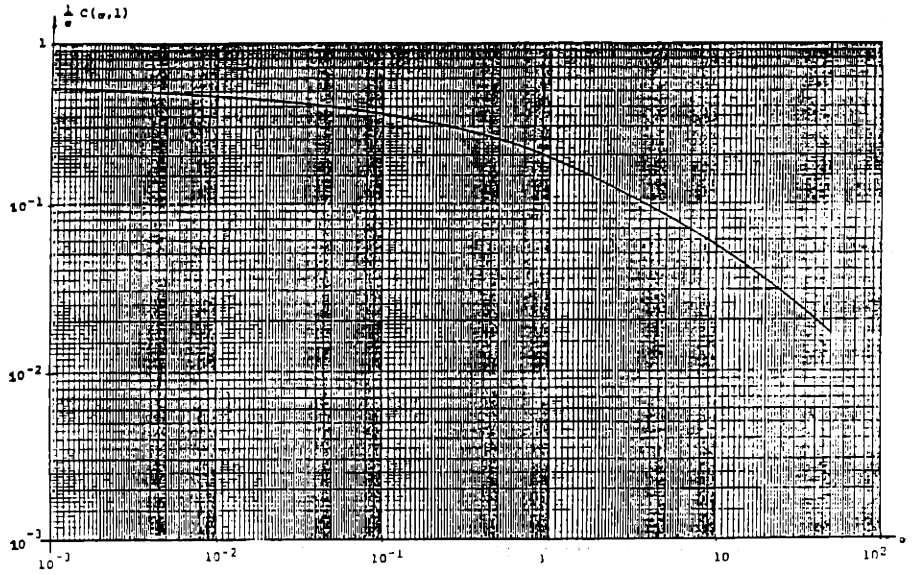

Figure 2.10: $\frac{C(a,1)}{a}$ *versus a.*

Finally, Richters concludes that, as long as the equal-eigenvalues assumption is made, numerical results can be obtained, while for the case of arbitrary $\underline{\lambda}$, there is no longer a guarantee that the optimum probability distribution is impulsive. He also noted that the lower bound presented here will be no longer valid for unequal eigenvalues.

2.4 Results and Interpretation

The results obtained previously are restricted to channels with K equal eigenvalues, and the discussion, summarized in what follows, referred consequently only to this type of channel.

2.4.1 Discussion of the Results

Significance of $p(x)$

The density $p(x)$ may be interpreted as the probability with which the letters for each code word (the modulation levels x_{mn}) are to be chosen at random. Since the optimum density consists of a finite set of impulses, this means that the input letters are chosen from a discrete set of levels. For small values of $a_o=P/N_oW$ two impulses were shown to be optimum, and this result is independent of the number of diversity paths. As a_o increases, two

impulses cease to be optimum, and more levels must be used to make best use of the increase in the amount of power available. On the other hand, if the rate is increased the number of levels also increases, since more levels are required to transmit the greater amount of information. One last observation to be mentioned here is that one impulse is always located at the origin.

Comparison with the Ideal Gaussian Channel

A comparison was done in Richters' report between the Rayleigh fading channel and the ideal Gaussian channel studied by Gallager, with an equivalent value of output signal-to-noise ratio per channel use.

The first major difference between the two channels is that the optimum density here was found to be impulsive while for the Gaussian channel it is continuous (Gaussian). In Fig. 2.11 a comparison of the respective exponents for the expurgated bound for $\rho=1$ and $\rho=\infty$ was reproduced. In Fig. 2.12 the equivalent capacities for the fading and non-fading channels are plotted versus a. It is clear from the plots that performance is always better for the Gaussian channel. On the other hand, although it does not appear clearly from the figure, the capacity of the infinite-bandwidth fading channel is known to be the same as that of an equivalent Gaussian channel.

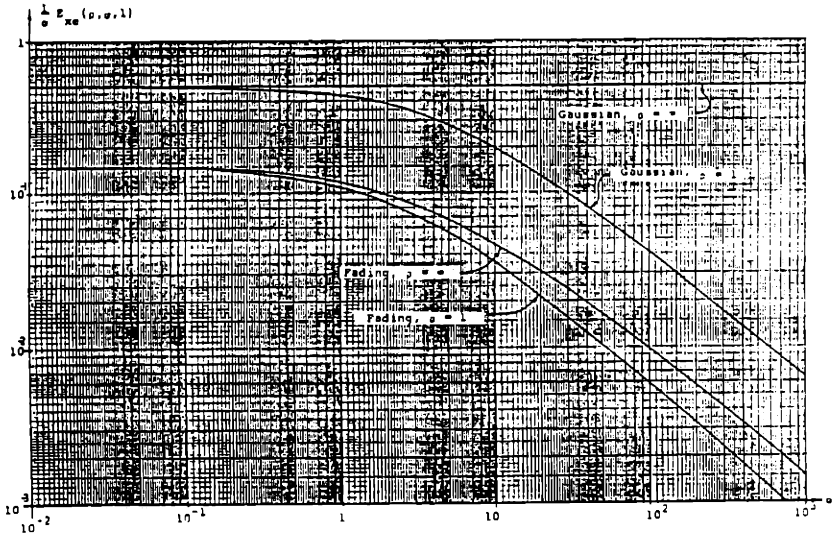

Figure 2.11: *Exponents for Equivalent Gaussian and Fading Channels.*

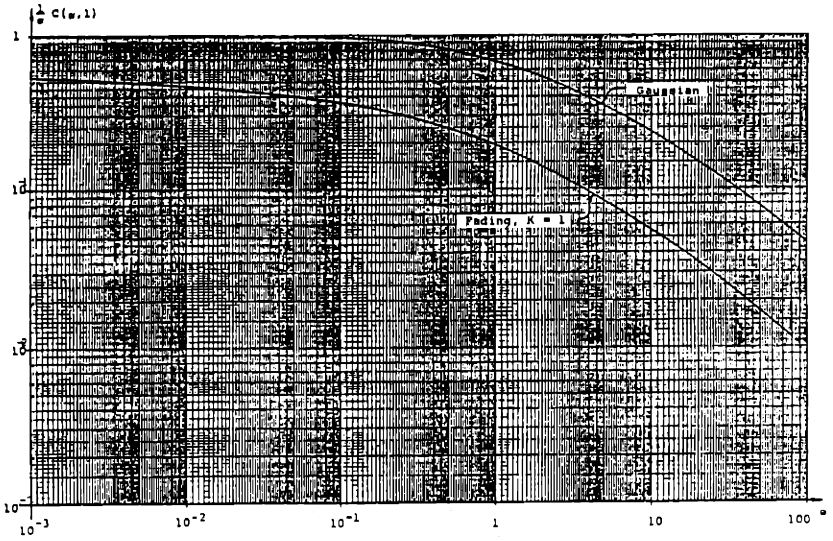

Figure 2.12: *Capacities for Equivalent Gaussian and Fading Channels.*

2.4.2 Application to the Communication Problem

Exponent-Rate Curves

In the previous section, the derived sphere-packing lower bound and the expurgated and random-coding upper bounds all had the same basic form, differing in subscripts and ranges of ρ, so the random coding bound will be considered typical, and application of this bound assuming ideal interleaving as described in Section 2.2 will be considered below.

Given the basic signals (in this model, just the specification of T_s and W_s), with the parameters B, L, W and P/N_o one may generate the exponent $E_{sc}(R)$, where

$$P_e \le e^{\left[\left(\frac{-PT}{N_o}\right)E_{sc}(R)\right]}.$$

The exponent $E_{sc}(R)$ is given by the upper envelope of the set of straight lines with slope (-ρ) and intercepts $E_{oe}[\rho, a_o(T_s+L)(W_s+B), K]/a_o(T_s+L)(W_s+B)$. K and $(T_s+L)(W_s+B)$ depend on T_s and W_s, and thus we are free to choose these quantities to obtain the largest exponents (subject to the rough constraint $T_sW_s \ge 1$). In general the maximization should be done numerically, but for some cases this was not necessary. At the end note that the interleaving gives the largest exponent of all the previously cited schemes.

Given R, the optimum value of ρ depends on T_s and W_s making the optimization difficult, and thus the procedure adopted, is to perform the maximization on T_s and W_s for several ρ's, draw the lines and get the resulting exponent numerically. This difficulty does not arise at the end points.

Zero Rate

The sphere-packing lower bound and the expurgated upper bound do not agree at this point (where $\rho=\infty$). As mentioned earlier, the zero-rate sphere-packing lower bound is not significant (for the DMC), since the zero-rate exponent of the expurgated bound is tight. Therefore, we will only examine Richters' results for the expurgated bound.

The optimization yields $(T_s+L)(W_s+B)/K=1$ for any $T_sW_s=1$ signal.

For the non-interleaving scheme, the optimal signals are found to be

$$T_s = \sqrt{\frac{L\alpha}{B}} \qquad W_s = \sqrt{\frac{B\alpha}{L}} \qquad \alpha \to \infty$$

As a practical matter, α does not have to be too large for the optimum exponent to be approximately attained.

When $BL \geq 1$, the interleaved and non-interleaved exponents are the same, while for $BL<1$, the non-interleaving bandwidth must be increased by a factor of $1/BL$ before the exponents are equivalent. This is explained by the fact that when $BL \geq 1$ both schemes are limited primarily by the guard space necessary to ensure orthogonality, but when $BL<1$, the non-interleaved scheme is penalized by the large guard spaces necessary for independence between output signals.

Capacity

The results simplify in this case because $\rho=0$ at capacity, independently of other parameters. It turns out that the optimum signal here satisfies

$$T_s = \sqrt{\frac{L}{B}} \qquad W_s = \sqrt{\frac{B}{L}} \qquad \text{for all } BL \tag{2.6}$$

with the resulting capacity

$$\frac{C_{sc}}{P/N_o} = \frac{C[a_o(1+\sqrt{BL})^2, (1+\sqrt{BL})^2]}{a_o(1+\sqrt{BL})^2}$$

Without interleaving, for all BL, the same signals were found optimum and the resulting capacity is

$$\frac{C}{P/N_o} = \frac{C[a_o(1+\sqrt{BL}+1/\sqrt{BL})^2, (1+\sqrt{BL})^2]}{a_o(1+\sqrt{BL}+1/\sqrt{BL})^2}$$

The capacity was computed previously only for the case when K=1 due to numerical difficulties, but since for many channels of interest $BL<10^{-1}$, the variation of C with K is believed to be not very large in the vicinity of K=1.

Other Rates

For the expurgated bound, the optimization is once again achieved by the signals of (2.6) for interleaving. For the case without interleaving, the optimization must be generally done numerically with the exception when BL is very far from unity.

For the random coding bound, the optimization can be done only numerically.

Comments

The general results Richters drew from the above study are:

1. The interleaving scheme is uniformly best, although for $BL \geq 100$, interleaved, non-interleaved schemes are about equivalent.

2. When $BL \leq 10^{-2}$, the non-interleaved scheme requires an increase in bandwidth by a factor of $1/BL$ to get the exponent attainable by interleaving.

3. For interleaving, the basic signals of (2.6) appear to be optimum. These signals with their associated guard space, take less space in the T-W plane than any others, which indicates that it is better to use many basic signals, each with a small amount of diversity than to provide more diversity per signal with a corresponding decrease in the coding constraint length.

   One should keep in mind however that no channel identification so ever was attempted in this report, and we believe these results will significantly change if some channel estimation is done.

4. When interleaving is considered, larger values of BL result in larger error probabil-

ities. Without interleaving, small values of BL are also bad because of the large guard spaces required for independence.

2.4.3 Numerical Examples

Among the few numerical examples that were provided at the end of the report, one studied how to generate an exponent-rate curve for the interleaving scheme on a channel with a value of $BL \leq 10^{-2}$. The basic signals of (2.6) were used, since they are optimum for the expurgated bound and capacity and thus believed to be "good". For a given value of P/N_o the resulting P_e was evaluated. A second example was considered and consisted of computing the bandwidth required to attain q ($0<q<1$) times the infinite bandwidth exponent.

2.5 Summary and Conclusion

In his report, J. Richters considered the transmission of digital information over a fading dispersive channel, subject to a bandwidth constraint on the input signals. He proposed a specific signaling scheme and modeled the problem as block coding over successive independent uses of a diversity channel. The main objective of the report was the derivation of a lower and upper bound on the minimum probability of error attainable by such a scheme, and then the investigation of some potential applications.

Some trends of channel behavior and performance were concluded in the report:

1. With the presented methods and results, it is possible to make some rough performance estimates for coding over reasonable signaling schemes.

2. For this type of signaling, except at zero rate or with an infinite available bandwidth, channels with $BL > 1$ are generally inferior to those with smaller values of BL.

   Obtaining a different result would have been very surprising. But again, this result while obvious when channel identification is used, is not so clear without it.

3. For $BL > 1$, there is little difference between interleaved and non interleaved signals, while in the opposite case, non-interleaved signals require an increase in bandwidth in order to obtain results comparable to the ones obtained by interleav-

ing.

Richters proposed future work on this problem along two fronts: analytical and numerical. Analytically, work may be done to relate the performance of the channels with arbitrary $\underline{\lambda}$ to that of the equal-eigenvalues channels for the random coding bound. It has also been suggested to find the true exponent for the zero rate. Numerically, Richters states that improvement can be made on the computations required for the random coding bound. As for the expurgated bound, it may be possible to obtain some results for arbitrary $\underline{\lambda}$.

Richters succeeded in his report in providing the insight he wanted to give to the reader. However, as we have already noted, the appendices of the report are highly mathematical in nature and contain all the derivations of the theorems used in the paper. The correctness of some of them is worth checking as it highly influences the nature of the results obtained. On the other hand, Richters failed to provide the important proof of the impulsive nature of the capacity achieving distribution.

We believe that the natural extension to Richters work is to try to find out whether the optimal distribution is really discrete, and if yes, find a simple proof of this result and characterize as completely as possible the optimal distribution. It was in this direction that we have pursued our research, and the results we have obtained are presented in the following chapter.

Chapter 3

The Capacity of an IID Rayleigh Fading Channel

As it was pointed out previously, in his report, Richters stated the Kuhn-Tucker conditions for the sought-after distribution, and solved numerically the equations within the set of finite discrete distributions. One wonders whether some "continuous" distributions can also be solutions, and even question the original assumption of the finite discrete character of the set where the minimization was done. Why is it assumed that the optimal distribution is discrete? What about the eventual numerical errors? Couldn't they lead to a wrong optimal distribution with a discrete character? In this chapter we will answer these questions by proving that the only possible distribution that satisfies the Kuhn-Tucker conditions is a discrete one, explaining therefore the procedure adopted by Richters, and finding the optimal distribution that was not provided in the original report.

In the following sections, we will prove the necessity of the discrete character of the capacity achieving distribution on the input levels. We will attempt next to find the locations of these mass points and prove that one of them is at zero. Finally, we will develop an algorithm and compute the optimal distribution numerically.

3.1 The Kuhn-Tucker Condition

Let's limit our study to the case $K=1$ (no diversity). Having an average power constraint $a=\mathrm{E}[X^2]$, we have proven in Appendix A that the capacity achieving input random variable X^*satisfies

$$\gamma(x^2-a)+C \geq \int_0^\infty p(y/x)\ln\left[\frac{p(y/x)}{p(y)}\right]dy \qquad \forall x \geq 0\,,$$

with equality if x is in the support of X^*. As derived in equation (2.3), the conditional prob-

ability density function of Y given X is

$$p(y/x) = \frac{1}{1+x^2} \cdot \exp\left(-\frac{y}{1+x^2}\right). \tag{3.1}$$

The solutions C and X^* of this equation are the capacity of the channel and a random variable that achieves it, respectively.

Since x appears in the above equations only via its square, it has been found useful and considerably easier to make the change of variables $s = \frac{1}{1+x^2}$. The Kuhn-Tucker condition can then be written as

$$\gamma\left(\frac{1}{s} - 1 - a\right) + C \geq \int_0^\infty s \cdot \exp(-s \cdot y) \ln\left[\frac{s \cdot \exp(-s \cdot y)}{p(y)}\right] dy \qquad \forall s \in (0, 1] .$$

By expanding the term inside the integral, the condition becomes

$$\gamma\left(\frac{1}{s} - 1 - a\right) + C - \ln(s) + 1 + \int_0^\infty s \cdot \exp(-s \cdot y) \ln[p(y)] dy \geq 0 . \tag{3.2}$$

Equation (3.2) will be referred to as "the Kuhn-Tucker condition".

3.2 The Discrete Character of X^*

Proving that X^* must be a discrete random variable is equivalent to proving that $S^* = \frac{1}{1+X^{*2}}$ is discrete. This is true because we have an invertible relationship between x and $s=1/(1+x^2)$ when x is restricted, as in our case, to be non-negative.

In the following section, using the same type of argument that was used previously by J. G. Smith [6] and later by S. Shamai and I. Bar-David [7], we will prove that having the support of S^* include a *positive* accumulation point is absurd. Therefore, the only two possibilities left are: either (1) to have S^* discrete with a finite number of mass points, and consequently X^* discrete and finite valued, or (2) to have S^* with an accumulation point only at zero, and consequently X^* discrete and infinite valued.

3.2.1 Assuming the Support of X^* Infinite

Assume in the following section that the support of X^* includes a *bounded* infinite set of

distinct points S_X, $S_X \subset [0, A]$. This can be the case for example if X^* has a density $p^*(x)$ that is positive on a set of non-zero measure. Since we have a one-to-one operator relating the random variables X^* and S^*, the support of S^* includes a set S_S, the image of S_X. The set S_S contains an infinite number of distinct points in the bounded interval $\left[\frac{1}{1+A^2}, 1\right] \subset (0,1]$, which implies that it has an accumulation point in (0,1] as shown in Appendix B.

Since the support of S^* has an accumulation point in (0,1], we can build a sequence $\{s_i\}$ of elements of S_S that converges to a point inside (0,1].

Define a function $h(z)$ in the complex variable z:

$$h(z) = \gamma\left(\frac{1}{z} - 1 - a\right) + C - \ln(z) + 1 + \int_0^\infty z \cdot \exp(-z \cdot y) \ln[p(y)] dy ,$$

where $\ln(z)$ is the principal determination of the logarithm [8]. Given this choice, the function $h(z)$ is analytical over the domain D defined by $\mathrm{Re}(z)>0$, for example.

On the interval (0,1] of the real axis, the Kuhn-Tucker condition (3.2) states that the function $h(z)$ is zero if z is in the support of S^*. Therefore, $h(z)$ is zero on the sequence $\{s_i\}$. We have thus an analytical function over a domain D that is zero over a sequence of distinct points converging inside the domain. The identity theorem [9] states that $h(z)$ is zero over the whole domain D.

Let's examine carefully the consequences of this result. The equation

$$\gamma\left(\frac{1}{s} - 1 - a\right) + C - \ln(s) + 1 + \int_0^\infty s \cdot \exp(-s \cdot y) \ln[p(y)] dy = 0 \quad \forall s \in D , \tag{3.3}$$

can be rewritten as

$$\int_0^\infty e^{-s \cdot y} \cdot \ln[p(y)] dy = -\frac{1}{s} \cdot \left[\gamma\left(\frac{1}{s} - 1 - a\right) + C - \ln(s) + 1\right] \quad \forall s \in D .$$

The left hand side is clearly the unilateral Laplace transform of the function $\ln[p(y)]$, while the right hand side can be written as:

$$-\frac{\gamma}{s^2} + \frac{1}{s} \cdot [\gamma(1+a) - C - 1] + \frac{1}{s} \cdot \ln(s) . \tag{3.4}$$

By adding Euler's constant C_E to the last term and subtracting it, equation (3.4) becomes:

$$-\frac{\gamma}{s^2}+\frac{1}{s}\cdot[\gamma(1+a)-C-1-C_E]+\frac{1}{s}\cdot[\ln(s)+C_E].$$

This is the Laplace transform of

$$-\gamma\cdot y+[\gamma(1+a)-C-1-C_E]-\ln(y).$$

The uniqueness of the Laplace transform for continuous functions of bounded variations over D (see [8]) implies that $\ln[p(y)] = -\gamma\cdot y+[\gamma(1+a)-C-1-C_E]-\ln(y)$. Therefore, the only possible output distribution satisfying (3.3) is of the form:

$$p(y) = K\cdot\frac{e^{-\gamma y}}{y}, \tag{3.5}$$

where $K = e^{\gamma(1+a)-C-1-C_E}$.

We can easily check that (3.5) gives indeed the general form of the solution by plugging it into (3.3). But for any value of K and γ, equation (3.5) is not a valid probability distribution, given that its integral over $(0,\infty)$ can never be finite.

3.2.2 Conclusion

We have assumed the support of X^* to include a *bounded* infinite set of distinct points. We have proven next using a complex analysis result that the Kuhn-Tucker condition is satisfied with equality over the entire set of potential inputs. By transforming the problem to an inverse Laplace transform problem, we have proven that the only possible output density satisfying the condition with equality is not a valid probability density.

This contradiction leads to the conclusion that the original assumption on X^* was wrong, and that the optimal random variable that satisfies the Kuhn-Tucker condition (3.2) can only be either discrete with a finite set of mass points, or infinitely discrete but with only a finite number of points in any bounded interval.

3.3 The Existence of an Impulse at Zero

Based on the previous analysis, we know now that the capacity achieving distribution is discrete with a *countable* number of mass points. The next natural task is to find where the mass points are located. Unfortunately, we were only able to find these locations numeri-

cally. However, in this section, we will prove by contradiction that the optimal input random variable X^* has necessarily a mass point at zero.

Because X^* is countably discrete, it has a density function $p^*(x)$ that can be written as $p^*(x) = \sum_{i \in I} p_i \delta(x - x_i)$, where the x_i's satisfy $0 \le x_0 < x_1 < \ldots$, and where I is either a finite set of the form $\{0, \ldots, L\}$ or the set of natural numbers $\mathbb{N}$. Assume now that X^* contains no mass point at zero, i.e. $x_0 > 0$. Let us fix the p_i's and $x_1, x_2, \ldots$ and move x_0 downwards.

By moving x_0 downwards, we are taking the inputs further apart, and intuitively we expect the probability of error in retrieving the input to decrease. One could think of unusual strange channels where for lower x_0 the uncertainty is spread at the output. But since our channel is "well behaved", we expect by decreasing x_0 to be able to send more information through the channel. Although this result seems intuitive, it has been found very difficult to obtain a proof inspired by this reasoning.

Clearly, the capacity is a non decreasing function of the power constraint (as we can always disregard the additional amount of power available). By fixing the p_i's, $i \ge 0$ and x_i's, $i \ge 1$, and moving x_0 downwards, the power constraint becomes obviously looser. Proving therefore that the mutual information increases is sufficient for proving that the original density is not optimal, given that we would have obtained, for a lower power constraint, a higher mutual information.

3.3.1 The Mutual Information

For a discrete input X, the mutual information between X and Y is

$$I(X, Y) = \sum_{i \in I} p_i \int_0^\infty p(y/x_i) \ln \left[\frac{p(y/x_i)}{\sum_j p_j p(y/x_j)} \right] dy .$$

If we differentiate $I(X,Y)$ with respect to x_0 we obtain:

$$\frac{\partial}{\partial x_0} I(X, Y) = p_0 \left[\int_0^\infty \frac{\partial}{\partial x_0} p(y/x_0) \ln \left[\frac{p(y/x_0)}{\sum_j p_j p(y/x_j)} \right] dy + \int_0^\infty p(y/x_0) \frac{\frac{\partial}{\partial x_0} p(y/x_0)}{p(y/x_0)} dy \right]$$

$$- \sum_{i \in I} p_i \int_0^\infty p(y/x_i) \frac{p_0 \frac{\partial}{\partial x_0} p(y/x_0)}{\sum_j p_j p(y/x_j)} dy ,$$

which simplifies to

$$\frac{\partial}{\partial x_0} I(X, Y) = p_0 \int_0^{\infty} \frac{\partial}{\partial x_0} p(y/x_0) \ln \left[\frac{p(y/x_0)}{\sum_j p_j p(y/x_j)} \right] dy . \tag{3.6}$$

To simplify (3.6) further, we differentiate (3.1),

$$\frac{\partial}{\partial x_0} p(y/x_0) = 2x_0 \left[-\frac{1}{(1+x_0^2)} + \frac{y}{(1+x_0^2)^2} \right] p(y/x_0)$$

$$= \frac{2x_0}{(1+x_0^2)^2} [y - (1+x_0^2)] p(y/x_0) ,$$

and define $f(y)=\ln[p(y/x_0)/p(y)]$, then

$$\frac{\partial}{\partial x_0} I(X, Y) = \frac{2x_0 p_0}{(1+x_0^2)^2} \int_0^{\infty} [y - (1+x_0^2)] p(y/x_0) f(y) dy .$$

***Theorem* 1**: *Let $p(y)$ be a probability density function with mean m. If $f(y)$ is a monotonically decreasing function then* $\int (y-m) p(y) f(y) dy < 0$.

Proof: *see Appendix C.* ■

To apply Theorem 1, notice that the mean of $p(y/x_0)$ is $(1+x_0^2)$. To show that $f(y)$ is monotone write

$$\frac{p(y)}{p(y/x_0)} = p_0 + \sum_{i \in I} p_i \frac{(1+x_0^2)}{(1+x_i^2)} e^{y\left(\frac{1}{(1+x_0^2)} - \frac{1}{(1+x_i^2)}\right)} .$$

Since $0<x_0<x_1< \ldots$, we have $1/(1+x_0^2)>1/(1+x_1^2)> \ldots$. Hence, all the exponents of the exponentials are positive so that the ratio $p(y)/p(y/x_0)$ –an average of increasing functions– is an increasing function. Therefore, the argument of the logarithm is decreasing and consequently so is the logarithm.

It follows that the derivative of $I(X,Y)$ with respect to x_0 is negative for $0<x_0< x_1$. This implies that, with the p_i's $i \geq 0$ andx_i's $i \geq 1$ fixed, $I(X,Y)$ is a decreasing function of x_0 and by moving x_0 towards zero we can achieve a higher mutual information.

3.3.2 Conclusion

We have started by assuming that the optimal distribution has no impulse at zero. We have shown next that the mutual information is a decreasing function of the location x_0 ($x_0 > 0$) of the closest impulse to the origin. Therefore, considering the same previous distribution with this impulse located at $x_0/2$ instead of x_0, would result in a higher mutual information, which contradicts the original assumption.

This leads to the conclusion that $p^*(x)$ has an impulse located at the origin: a very intuitive result since a zero level input is "good" for the power constraint and results in the smaller variance at the output and should be preferred to other levels.

3.4 Assumption

It has been shown in Section 3.2 that the capacity achieving distribution is discrete and can only have one of two forms: either discrete with a *finite* number of mass points, or with infinite number of mass points but such that *only a finite* number of them is in any bounded interval. We strongly believe that it is possible to rule out the second possibility, although we were not able to provide an analytical proof for this result, given the short time frame available. Intuitively, one can argue that having an infinite number of impulses that go to infinity is not necessarily better than a finite number. Having input levels going to infinity is clearly "good" for detection and decreases $h(X/Y)$. But on the other hand, the power constraint obliges the probabilities of these impulses to go to zero "very fast". This uneven distribution on the input levels is "bad" for the input entropy function $h(X)$. Therefore, one can possibly do better with an alternative input distribution that uses a finite number of impulses, but with a more uniform distribution on the inputs. Note finally that cutting out the impulses that go to infinity is also better for the power constraint.

Hence, for all practical purposes, we are going to assume in the rest of this study that the optimal probability distribution is discrete with a *finite* set of mass points.

3.5 Numerical Results

Having characterized as completely as possible the optimal probability distribution, we can now compute numerically the capacity of an IID Rayleigh fading channel as a function of the power constraint. This was attempted previously by Richters in his report [1], but much more powerful numerical techniques and computational tools are available nowadays and more precise results may be obtained. Moreover, the capacity achieving distribution was not provided in Richters' work, and how this distribution varies as a function of the power constraint is of great interest. Another intriguing aspect we would like to study based on these simulations is the behavior of the optimal distribution when the power constraint is very low.

Our optimization problem is the following: we would like to maximize the mutual information $I(X,Y)$ over the input probability density, given an average power constraint. The usual approach to such a maximization is to use a Lagrange multiplier (as shown in [10]), say ρ, and to maximize $J(\rho)=I(X,Y)-\rho E[X^2]$ over all choices of the set of input probabilities. This approach is dual to the widely known rate-distortion curves drawing method [2], and similarly, as it is interpreted in the rate-distortion case, the multiplier ρ has here also the geometric significance of being the magnitude of the slope of the curve $C(a)$ at the point generated by that value of ρ.

Indeed, let's consider in Fig 3.1 plotting $I(X,Y)$ and $E[X^2]$ for any particular input probability distribution, on a graph with ordinate I and abscissa $E[X^2]$. A line of slope ρ through this point will intercept the I axis at $I(X,Y)-\rho E[X^2]$. The distribution that maximizes $J(\rho)$ will maximize that I axis intercept, and all points on the $C(a)$ curve will lie on or below the line of slope ρ through this intercept. Thus, this line is tangent to the $C(a)$ curve. Consequently, $0<\rho\leq 1$.

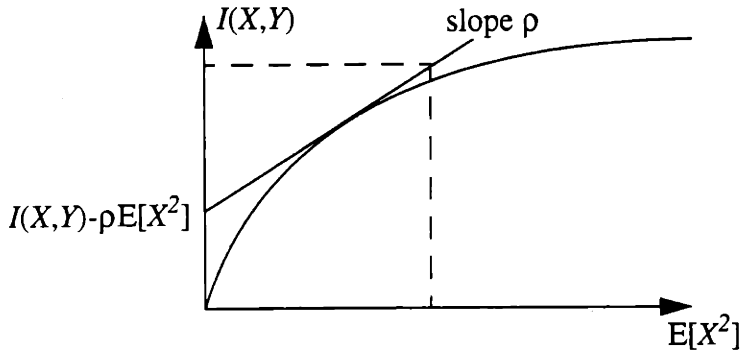

Figure 3.1: *The Slope ρ of the Curve C(a)*

We have already assumed that the optimal probability density is discrete with a finite set of mass points, which facilitates our task by looking for the optimal distribution in the set of discrete ones. The maximization problem can therefore be stated as follows: maximize $J(\rho)=I(X,Y)-\rho E[X^2]$ over $p_0 \ldots p_N$ and $x_1 \ldots x_N$, subject to the following constraints: the x_i's ≥ 0 and the p_i's lie in the simplex S defined by $p_i \geq 0$ and $\sum_{i=0}^{N} p_i = 1$. The sought-after graph is then drawn by varying the parameter ρ.

3.5.1 The Algorithm

The set of constraints, as defined earlier, is clearly a convex set (intersection of two convex sets). However, since the maximization over the locations and probabilities is clearly non-linear, a projected gradient descent method was used.

The algorithm under its most general form is the following:

1. Choose an arbitrary initial vector $v^0=(x_1, \ldots, x_N, p_0, \ldots, p_N)$ that lies in the set of constraints.
2. Let $v^{n+1} = P(v^n - \alpha^n \nabla J(v^n))$, where P is the orthogonal projection operator onto the set of constraints, α^n the step size for iteration n, and ∇J the gradient of our functional J.
3. Repeat step 2 until the norm of $\nabla J(v^n)$ is less than a given threshold.

3.5.2 The Gradient

The gradient of J is given by:

$$\nabla J = \left(\frac{\partial}{\partial x_0}J, \ldots, \frac{\partial}{\partial x_N}J, \frac{\partial}{\partial p_0}J, \ldots, \frac{\partial}{\partial p_N}J\right)$$

$$\text{where } \frac{\partial}{\partial x_i}J = p_i\int_0^\infty \frac{\partial}{\partial x_i}p(y/x_i)\ln\left[\frac{p(y/x_i)}{\sum_j p_j p(y/x_j)}\right]dy - \rho p_i(2x_i),$$

$$\text{and } \frac{\partial}{\partial p_i}J = \int_0^\infty p(y/x_i)\ln\left[\frac{p(y/x_i)}{\sum_j p_j p(y/x_j)}\right]dy - 1 - \rho x_i^2 .$$

3.5.3 The Step Size

The step size can be made optimal by computing the Hessian of the functional J. These computations were found very complex and beyond the scope of this study, so a fixed step size was chosen for all the iterations: $\alpha^n = \alpha \ \forall n$.

We have the following result [11]: Let M be an upper bound to the norm of the Hessian over the set of constraints. For $0<\alpha<2/M$ the projected gradient method converges.

As it was pointed out previously, computing M has been found very difficult and we have relied on experiments to find the suitable value for the step size α.

3.5.4 The Projection

By simple examination of the type of constraints we have in this problem, one can see that they can be separated independently into two parts: one dealing with the x_i's being positive, and the other with the fact that the p_i's lie in the simplex S.

Concerning the positions, the orthogonal projection is simply given by the following rule: if an x_i is negative, then make it zero. Otherwise, do not change it.

As for the probabilities, the projection rule is much more complex: it can be divided into two parts. First, project on the hyperplane defined by $p_0 + \ldots + p_N = 1$, and next inside the hyperplane, find a rule to project on the simplex.

Projection on the Hyperplane

A unitary vector that is orthogonal to the hyperplane is $\left(\frac{1}{N+1}, \ldots, \frac{1}{N+1}\right)\sqrt{N+1}$. Since the

distance from the origin to the hyperplane is $\frac{1}{\sqrt{N+1}}$, the projection is given by:

$$\boldsymbol{p} - \left[\sqrt{N+1}\cdot\frac{\left(\sum_{i=0}^{N} p_i\right)}{N+1} - \frac{1}{\sqrt{N+1}}\right]\sqrt{N+1}\begin{pmatrix}\frac{1}{N+1}\\ \vdots \\ \frac{1}{N+1}\end{pmatrix} = \boldsymbol{p} - \left[\left(\sum_{i=0}^{N} p_i\right) - 1\right]\begin{pmatrix}\frac{1}{N+1}\\ \vdots \\ \frac{1}{N+1}\end{pmatrix}.$$

Projection on the Simplex

Being now on the hyperplane H: $p_0 + \ldots + p_N = 1$, we need to specify a rule for the projection on the simplex S ($p_i \geq 0$ and $\sum_{i=0}^{N} p_i = 1$) lying in that hyperplane.

Consider an arbitrary point $\boldsymbol{p}^0$ on the hyperplane. Let I be the set of the indices of the positive components of $\boldsymbol{p}^0$: $I=\{0\leq i\leq N,\ p^0{}_i>0\}$ and L its cardinal. Let's project first on the boundary B of the simplex contained in the set $\{p_i=0\ i\notin I\}$ as shown on Fig 3.2. The equation of B is given by $\sum_{i\in I} p_i = 1$.

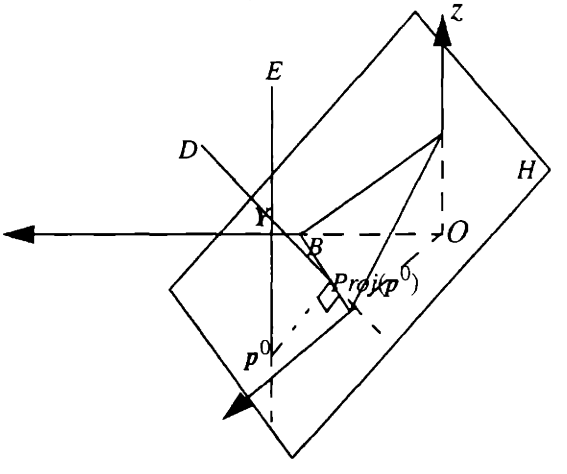

Figure 3.2: *Projection on the Simplex in 3D*

Note that the set $E = \{p_i=p^0{}_i,\ i\in I\}$ (parallel to Oz in Fig. 3.2) intersects with the orthogonal line D passing through the point $Proj(\boldsymbol{p}^0)$ of boundary B where $\boldsymbol{p}^0$ should be projected.

Let's call $\boldsymbol{Y}$ this intersection point. We have $\boldsymbol{Y} - Proj(\boldsymbol{p}^0) = \alpha \begin{pmatrix} 1 \\ \vdots \\ 1 \end{pmatrix}$ for some α. Since $Y_i = p^0{}_i$ for $i \in I$, by direct identification we find that

$$Proj(\boldsymbol{p}^0)_i = p_i^0 - \frac{\sum_{i \in I} p_i^0 - 1}{L} \qquad (i \in I)$$

$$Proj(\boldsymbol{p}^0)_i = 0 \qquad (i \notin I)$$

Some components of the projection $Proj(\boldsymbol{p}^0)$ may be negative, which means that they lie on the boundary but outside the simplex. In this case, the above procedure is repeated with $\boldsymbol{p}^0$ replaced by $Proj(\boldsymbol{p}^0)$. We keep iterating these projections until one gets to the boundary of the simplex. This happens when all of the components of $Proj(\boldsymbol{p}^0)$ are non-negative.

After each iteration the cardinal L of the set I of the positive components of the probability vector does not increase. This can be seen by noticing that the non-positive components of the vector are all set to zero, while some of the positive components might become non-positive. If the value of L from one step to the next does not decrease, this means that all the components of $Proj(\boldsymbol{p}^0)$ are non-negative and clearly the algorithm stops. On the other hand, if the value of L decreases it will decrease by at least one. Given that L is lower bounded by one, it is guaranteed that this procedure will converge.

3.5.5 The Number of Impulses

Since we have argued in Section 3.4 that we suspect the optimal input distribution to be discrete with a finite number of mass points, one would expect to have as few as two points for low values of SNR, and this number increases as the power constraint becomes higher.

The numerical simulations have confirmed the sufficiency of two points for low values of a, and that the number of points increases, as expected, when a increases. We believe it is possible to prove analytically the sufficiency of two points in the neighborhood of zero, but we have been contented with the computational result. For a very low average power constraint, we start with an initial density having three impulses and then we see two merge into one, or just the probability of one of them getting to zero, proving that the

actual density has only two mass points. On the other hand, when we increased the power constraint, we found the optimal density to have more and more impulses.

In order to avoid running the program using additional points that will turn out not useful later, we have derived in the following section a condition which, when satisfied, implies that an additional impulse is needed.

When an Additional Impulse is Required

The analysis in this section is heavily inspired by a previous work done by K. Rose [12] in the context of rate-distortion theory. In what follows, we will mention the guidelines of Rose's work and develop analogous results for our problem.

A new approach, theoretically equivalent to the traditional approach (the Blahut-Arimoto algorithm), was developed by Rose in his paper. While the traditional approach is based on optimizing over the input density (the output density in the rate-distortion case), the new approach, called "the mapping approach", is based on searching for the optimal mapping x: $[0,1] \rightarrow X$, from the unit interval with the Lebesgue measure, denoted by μ, to the input space (an approach that is clearly equivalent to writing the problem in terms of the cumulative distribution function as a measure). Writing the functional J in this form we get

$$J(x)= \int_{[0,1]} \left(\int_0^{\infty} p(y/x(t)) \ln \left[\frac{p(y/x(t))}{\int_{[0,1]} p(y/x(u)) d\mu(u)} \right] dy - \rho x^2(t) \right) d\mu(t) \ .$$

The necessary condition for optimality obtained by applying the standard procedure in variational calculus, is given by

$$\frac{\partial}{\partial \varepsilon} J(x + \varepsilon \eta)|_{\varepsilon = 0} = 0 \text{ for all admissible perturbation functions } \eta(t). \qquad (3.7)$$

The necessary conditions obtained for the rate-distortion curve in Rose's paper were found similar to some statistical mechanics quantities, and an analogy was established with the well-known phase transition problem, which has helped finding the curve efficiently and characterizing the way discrete reproduction mass points were added. As explained in [12], an additional point is required when the optimal mapping stops defining the minimum of the free energy, and becomes a saddle point. This translates in our problem to the

following: at the critical ρ, the mapping satisfies the necessary condition (3.7), but there exists a particular perturbation $\eta(t)$ for which $\frac{\partial^2}{\partial\varepsilon^2}J(x+\varepsilon\eta)|_{\varepsilon=0} = 0$. Using the fact that the optimal distribution is discrete, we prove in Appendix D that this condition translates to the following: an additional impulse is needed when some point of support x satisfies both (3.7) and

$$\int_0^\infty \frac{\partial^2}{\partial x^2}p(y/x)\ln\left[\frac{p(y/x)}{p(y)}\right]dy + \int_0^\infty \left(\frac{\partial}{\partial x}p(y/x)\right)^2\left[\frac{1}{p(y/x)}\right]dy - 2\rho = 0\,, \tag{3.8}$$

$$\text{where } \frac{\partial}{\partial x}p(y/x) = 2x\left[-\frac{1}{(1+x^2)} + \frac{y}{(1+x^2)^2}\right]p(y/x)\,, \text{ and}$$

$$\frac{\partial^2}{\partial x^2}p(y/x) = \left(\frac{8x^2}{(1+x^2)^2} - \frac{2}{(1+x^2)}\right)p(y/x) + \left(\frac{-16x^2}{(1+x^2)^3} + \frac{2}{(1+x^2)^2}\right)yp(y/x) + \frac{4x^2}{(1+x^2)^4}y^2p(y/x)\,.$$

Therefore, we have adopted in our algorithm the following procedure: start with a high value for the parameter ρ (which corresponds to low values of a) with two points after checking that two are enough for that ρ. Then decrement ρ gradually, checking whether we need an additional mass point or not.

To Split or not to Split

One concern is whether mass points are added in a "splitting" fashion or they just appear in certain locations away from the existing ones (see Fig. 3.3).

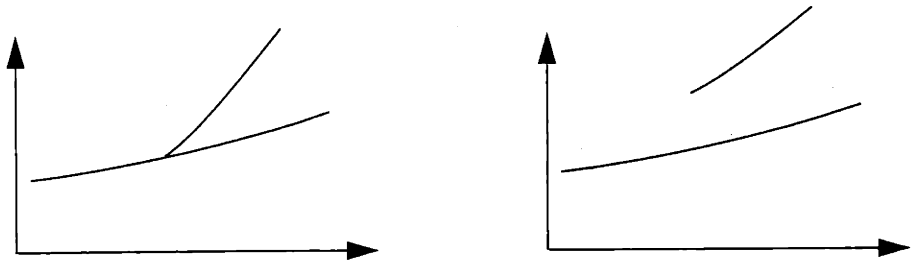

Figure 3.3: *Splitting vs. Non-Splitting*

We favor initially the splitting possibility inspired by the results K. Rose has obtained in his paper [12] for his problem. Based on the very well know similarities found between our problem and Rose's problem we conjecture to have a similar type of results, especially dealing with the splitting character of the input density: by a similar reasoning, the conti-

nuity of the $C(a)$ curve suggests that the system undergoes continuous transitions, which are symmetry breaks. This suggests that the mass points are added in a "splitting" way, in the sense that for some value of the parameter, one of the mass points splits in two separate points.

In the following sections we will see that the results do not conform to this initial guess, and we will intuitively analyze why.

3.5.6 Final Algorithm

The structure of the final algorithm is the following

1. Pick an arbitrary initial density with two mass points, and a small enough parameter ρ.
2. Perform the projected gradient method.
3. Compute the power and capacity and store the optimal distribution.
4. Check condition (3.8). If true, add an additional mass point x_{N+1}.
5. Decrement ρ.

3.5.7 Results and Analysis

The previously described algorithm was implemented in C programming language, and the results are shown in what follows.

Capacity of the Channel

In this section we will present the numerical results we have obtained for the capacity of the IID Rayleigh fading channel and the corresponding optimal distribution.

Figure 3.4 shows the capacity of the IID Rayleigh fading channel C, as a function of the power constraint a. An interesting comparison to study is between this fading channel and the non-fading ideal Gaussian channel. Such a comparison is done in a following subsection.

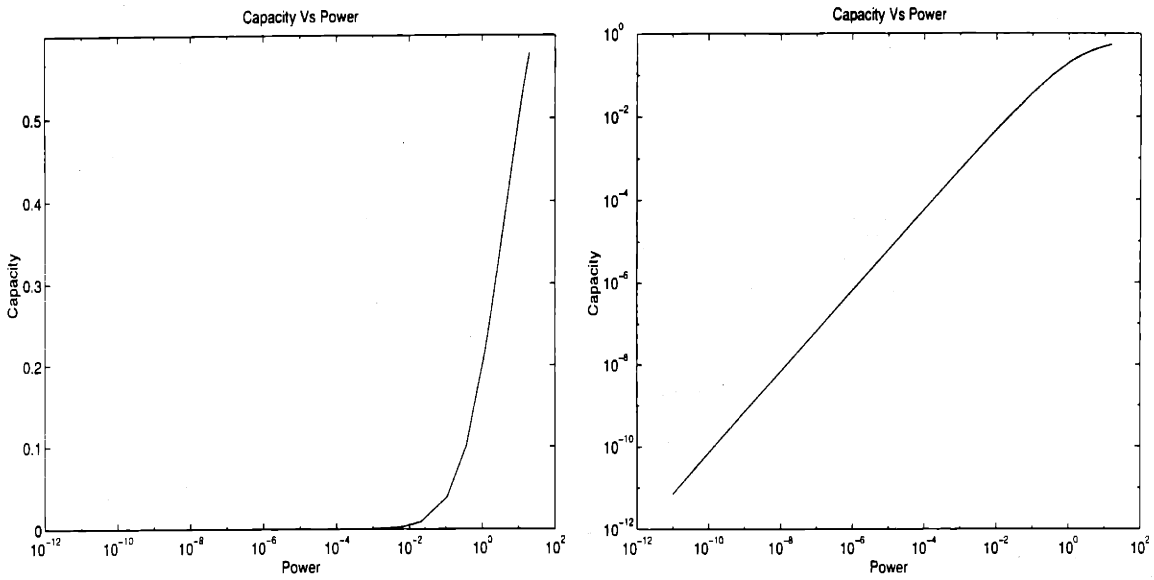

Figure 3.4: *Capacity versus Power*

Figures 3.5 and 3.6 show the locations and the probabilities of the optimal distribution we found to achieve capacity. The details of these graphs for low values of SNR will be studied separately in an upcoming subsection.

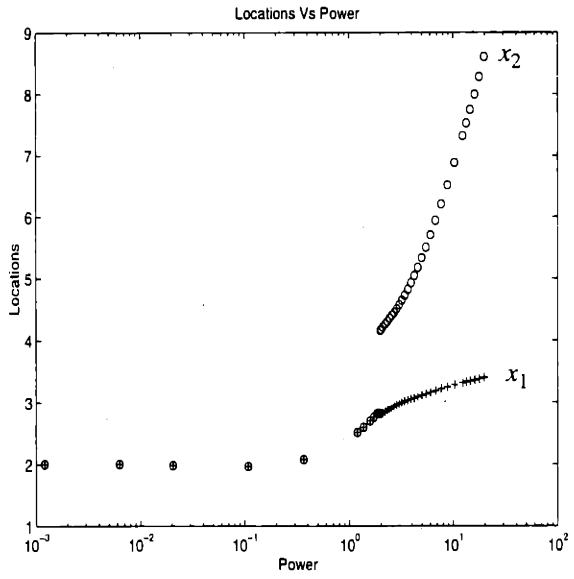

Figure 3.5: *Optimal Locations versus Power*

Note from this graph that the locations, after initially decreasing for very low values of a, uniformly increase as the power increases. We conjecture that the additional impulse to appear next will be between x_1 and x_2 since we expect intuitively to have the locations rel-

atively uniformly spread. Unfortunately we were not able to locate this impulse for reasons that will be discussed in the splitting section. Note that the graph is drawn on a semilogarithmic scale, so that the slope of the curve of x_2 is not as sharp as it initially appears.

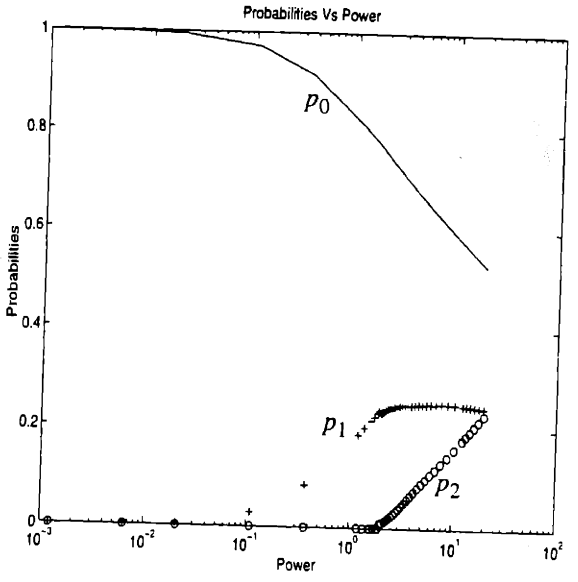

Figure 3.6: *Corresponding Optimal Probabilities*

Figure 3.6 shows the probabilities of the impulses of the optimal probability distribution. Note that, when the third impulse appears, its probability seems to grow on the expense of p_1: a similar result to what Richters has obtained for the optimal density for the expurgated bound. There is however a difference between these results and his. In our case, p_1 continues to increase after the addition of the new third impulse, while in Richters' report, p_1 decreases sharply after the appearance of the third impulse. Again, it is unfortunate that we were not able to locate the fourth impulse that will appear for higher values of a, in order to be able to characterize more completely the behavior of these probabilities. We suspect that p_1 will decrease later with a.

One last concern that needs to be discussed is whether the probabilities on this graph cross or not. Given that the entropy of the input distribution is not changed by permuting the probabilities of the impulses, one would expect initially to see the probabilities of the lower impulses higher than the probabilities of the high locations. This is due to the fact that this configuration is better for the power constraint. But on the other hand, for the

three impulses example, if the impulse at zero and the highest impulse are used more often than the middle one, one would expect the probability of error in retrieving the input at the output to decrease. Hence, there is a trade off between lowering the average power of the input and using the furthest apart impulses as often as possible, and predicting whether the curves in Figure 3.6 cross or not seems to be a complex matter.

Splitting

As suggested in Fig. 3.5, it appears that additional impulses are added in a non-splitting fashion. When the condition for adding an impulse is satisfied, an additional impulse appears far from the locations of the already existing impulses. This result, although agrees with Richters optimal density for the expurgated bound, was unexpected. Given that our problem is dual to the rate-distortion curve drawing problem, we initially expected the optimal density to behave similarly to Rose's optimal density [12] as a function of a. There is however a potential interpretation to this result. On one hand, making the inputs as separate as possible improves detection by decreasing the probability of error in recovering the inputs, and consequently, one would try to take the inputs as further apart as possible. This corresponds analytically to saying that $h(X/Y)$ decreases if the inputs are taken further apart. But on the other hand, given that the power is constrained to be less than a, taking the inputs further apart is done on the expense of the probabilities. This results in a decrease in the entropy function $h(X)$. Therefore, since $I(X,Y) = h(X)$-$h(X/Y)$, the optimal distribution that maximizes $I(X,Y)$ is seen to be the result of this equilibrium between the desire of taking the inputs as further apart as possible, and having to make the input density as close to a uniform density as possible. This trade off is believed to be at the origin of the "non-splitting" behavior of the optimal density.

Condition (3.8) derived previously has been found to be accurate as to predict when an additional impulse is needed. However, since the impulses are added in a non-splitting fashion, it has been found difficult to locate the additional impulse. This difficulty made the graph very hard to complete beyond the range used in the above figures. Condition (3.8) is satisfied at the end of this range, but we were not able to locate the additional impulse in the short time frame available. It would be very interesting to see whether this fourth impulse appears in between x_1 and x_2, or beyond x_2. We favor the first hypothesis.

Low SNR

For low values of a, it has been found that only two mass points were sufficient. This result has been obtained by starting with more than two points, and then finding that some of them merge and the probability of some others go to zero, and only two non-zero mass points were left.

As a decreases, the probability of the non-zero impulse goes to zero as it is shown on Fig. 3.7. On the same figure we have drawn the location of the non-zero impulse versus a. As expected we see that, as a gets smaller, x_1 increases. This suggests that, as less and less power is available, we ought to use higher and higher levels of input, less and less frequently. This level goes eventually to infinity as a goes to zero. However, as we can notice from the graph, the rate at which x_1 increases when a decreases is very low.

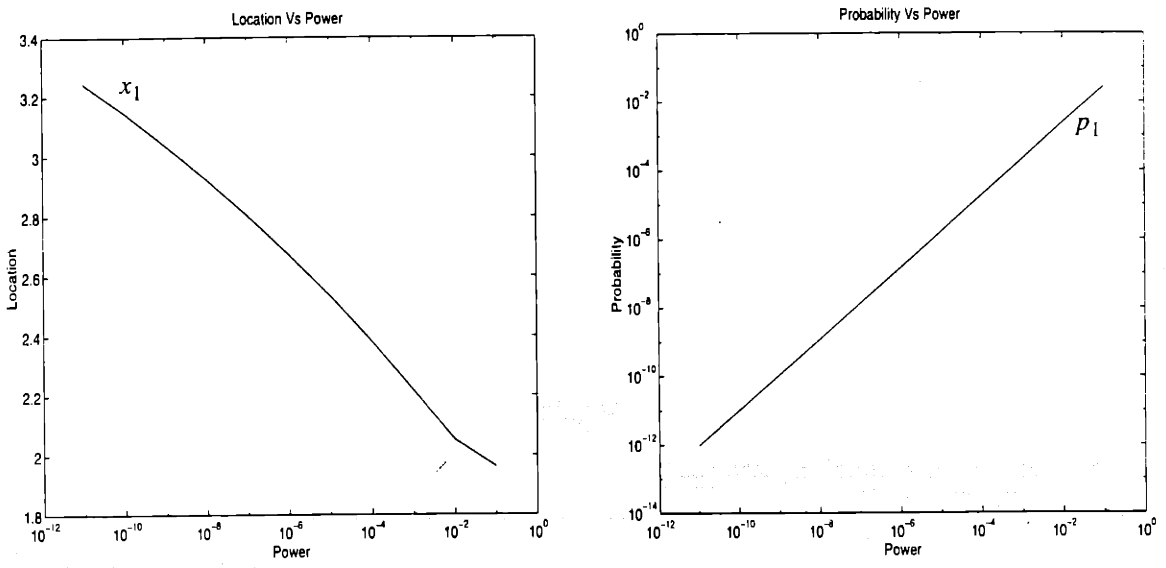

Figure 3.7: *Probability and Location of the Non-Zero Impulse.*

Comparison with the Ideal Gaussian Channel

In this section, a comparison is drawn between the IID Rayleigh fading channel, object of our studies, and the ideal additive white Gaussian noise channel with an equivalent value of signal to noise ratio. The major difference is in the form of the optimal distribution: in our case, it is an impulsive density where for the Gaussian channel, the optimal $p(x)$ is Gaussian. Before exposing the numerical results we have obtained, we expect the two

channels to behave identically for very low SNR's since it is known that the capacity of the infinite bandwidth fading channel is the same as that of an equivalent Gaussian channel.

Figure 3.8 shows equivalent capacities for the Rayleigh fading channel, and the non-fading channel. It is clear from these graphs that performance is always better for the Gaussian channel.

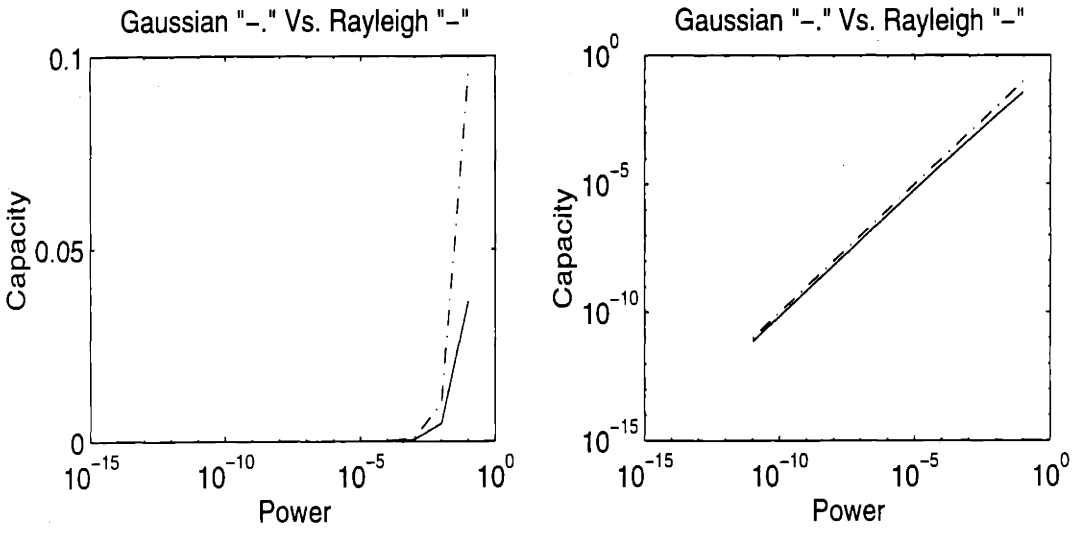

Figure 3.8: *The Fading Channel Compared to the Gaussian Channel.*

On Fig 3.9 the ratio of the capacity of the Gaussian channel to the capacity of the fading channel is drawn versus the power constraint. As we expect this ratio goes to 1 when $a \rightarrow 0$, but note the very slow rate of approach to this asymptote.

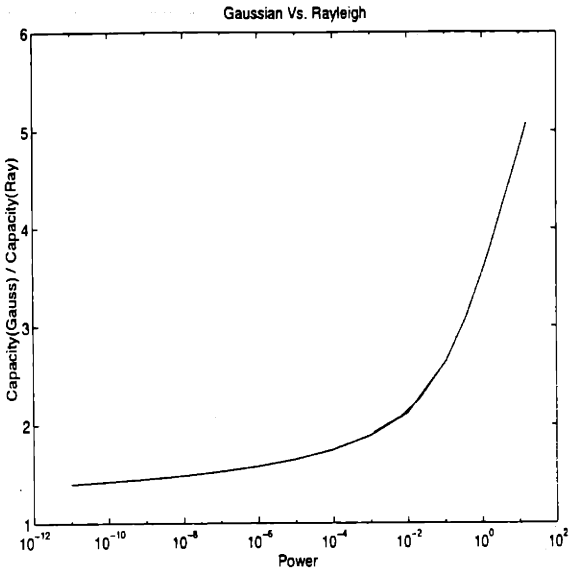

Figure 3.9: *The Ratio of Capacities.*

3.5.8 Conclusion

Although the program we have developed in this study is much faster than the traditional Blahut-Arimoto (BA) algorithm, it was found to have a poor performance given that it was very hard to locate the impulses when they appear. Our initial guess of the "splitting" character of the optimal probability distribution was misleading and suggested that the new algorithm will be much more efficient. This wrong initial guess hid this major drawback of the program.

We believe that a combination of the two algorithms (the BA algorithm and the one exposed in this thesis) would be a smart solution to our problem. An initial run of the BA algorithm would approximately locate the potential mass points, and a second run of the new algorithm would find the optimal distribution in a short time.

Another alternative algorithm is an "adaptive BA algorithm" where the grid is recursively adapted to the probabilities. This method will considerably reduce the size of the grid in the traditional BA algorithm.

Chapter 4

Summary and Conclusions

We shall briefly summarize the major points of this research and mention some possibilities for further work on the problem.

4.1 Summary

In the first part of this thesis, we have studied previous work done in the field of transmission over Rayleigh fading channels. We have focused our study on a report by J. Richters [1], and tried to understand it and find the motivation for what can be added to the field. Richters' report has provided us with the insight to the communication problem over fading channels subject to bandwidth and power constraints. Ideas were drawn on how to extend and complete what has already been achieved in this field, and we found the motivation to study first the IID Rayleigh fading channel. A summary and analysis of Richters' report was conducted in Chapter 2.

In the second part, we have started with Richters' numerical result that the capacity achieving distribution on this type of channels is discrete, and tried to prove this result. Inspired by some previous work done by Smith [6], Shamai and Bar-David [7], and Rose [12], in Chapter 3 we have proven that result and tried to characterize the optimal distribution. We have developed next an algorithm for computing the capacity and the corresponding optimal distribution function of the power constraint, and implemented it. The results obtained were analyzed in the last section of this chapter.

The major achievements we have made in this research are:

1. Proving that the capacity achieving distribution of an IID Rayleigh fading channel is discrete.

2. Proving that this optimal density has an impulse at zero.

3. Developing a numerical algorithm for computing the capacity of this channel, faster than the classical Blahut-Arimoto algorithm.

4.2 Future Work

There are openings for more work on this problem along many fronts. The most immediate one is studying the IID Ricean fading channel, and trying to find an analogous result for this type of channels. The Ricean model is appropriate when some information about the channel is known at the transmitter. We conjecture that, similarly to the Rayleigh case, the optimal distribution will be discrete, and a proof following the guidelines derived in this thesis might be promising.

Another important and challenging extension is to generalize the study to the non-IID Rayleigh fading case. As explained above, the IID-fading assumption is very limiting and polemic. On a slowly fading channel, Richters uses interleaving in order to obtain the IID-fading assumption, while one ought to estimate the channel and use the estimate. We expect some of the desired results to be very difficult to obtain. Here again, as a next step, one could try to generalize the study to non-IID Ricean fading channels.

Even if the above generalization is successful, it is likely that the conditions needed to achieve capacity are difficult to realize or simply not practical. Moreover, the random coding argument does not provide a practical way of coding that achieves capacity. Therefore, a third possibility is to study a simple suboptimal coding/decoding technique that appears to be promising: interleaved variable-rate codes. This scheme performs channel identification via information-bearing pilot tones. A pilot tone usually carries a fixed signal known by the receiver who uses it in order to get the desired estimate. An idea that has not been carefully considered in the literature is to have the pilot tone carry information. One would expect that with a power level high enough to determine the information sent even without prior knowledge of the channel, one could make a correct decision and then estimate the channel. From this perspective, one should expect to get relatively good results with a low rate code using non-coherent detection techniques such as On-Off-Keying. Is it feasible? What is the cost of such a technique? What's the highest achievable rate? And what's the

best way of realizing it? Trying to answer these questions via a thorough analysis of coding using this technique is an additional problem that can be worked on.

Studying these different problems comes under a general goal of understanding how the time-variant channel differs from the time-invariant one. One would like to obtain some qualitative results: under what fading conditions is the capacity close to the capacity of the Gaussian channel? How does the transition behave? For example, as the coherence time increases we intuitively expect to go from a Rayleigh fading channel to a Gaussian channel.

An interesting application of this study is shallow water acoustic communication. In the underwater environment, communication appears to be on the border of these two cases. One would like to obtain "good" schemes for reliably and efficiently communicating in this environment.

Appendix A

The Kuhn-Tucker Condition

A.1 The Maximization

Let us discuss first the maximization of the mutual information I over the input probability distribution subject to a power constraint.

The maximization is *achieved* by a *unique* probability distribution. The existence and uniqueness of the maximum is guaranteed because

1. The set of input distributions satisfying an average power constraint is convex and compact in the Levy metric topology.

2. The mutual information I is strictly concave, continuous, and weakly differentiable.

These results have been proven by Smith [6], and Shamai and Bar-David [7].

A.2 The Generalized Kuhn-Tucker Theorem

The generalized Kuhn-Tucker theorem [10] requires the following conditions to be satisfied:

1. The set X over which the maximization is done should be a vector space.

2. The functional to optimize should be Gateaux differentiable and real-valued.

3. The constraints seen as a mapping from X to a normed space Z should be Gateaux differentiable and linear.

4. The space Z should have a positive cone containing an interior point.

In order to apply this theorem note that the mutual information between the input X and the output Y is given by

$$I(X, Y) = \int_0^\infty \left(\int_0^\infty p(x)p(y/x) \ln \left[\frac{p(y/x)}{\int_0^\infty p(u)p(y/u)du} \right] dy \right) dx .$$

This way of writing the equation is somewhat ambiguous since $p(x)$ is in general a distribution that may not be associated to a function. Let's denote P this input probability distri-

bution and $P(h(x))$ the real value obtained from applying P to $h(x)$ (which is $E[h(X)]$). Therefore,

$$I(X, Y) = P\left(\int_0^\infty p(y/x)\ln\left[\frac{p(y/x)}{P(p(y/u))}\right]dy\right).$$

We would like to maximize $I(X,Y)$ over all possible input distributions P subject to the following constraints: $P(1_{[\alpha,\alpha+\beta]}) \geq 0\ \forall\alpha\geq 0$ and $\forall\beta\geq 0$, $P(1)=1$, and $P(x^2)-a \leq 0$, where the function 1_I of x takes the value one when x is in interval I and zero elsewhere. These constraints are the translation of what we can usually write as $\int_0^\infty p(x)dx = 1$, $\int_0^\infty x^2 p(x)dx \leq a$.

Since all of our functions have their support included in $[0,\infty)$, we have omitted multiplying by the function $1_{[0,\infty)}$ for clarity purposes, and it would be used as such throughout.

The set of distributions is a vector space and Condition 1 of the generalized Kuhn-Tucker theorem is satisfied. Conditions 2 is also satisfied and the Gateaux differential of I with respect to P is

$$\begin{aligned}
\partial I(X,Y,P+\lambda\eta)/\partial\lambda_{|\lambda=0} &= \eta\left(\int_0^\infty p(y/x)\ln\left[\frac{p(y/x)}{P(p(y/u))}\right]dy\right) - P\left(\int_0^\infty p(y/x)\left[\frac{\eta(p(y/u))}{P(p(y/u))}\right]dy\right) \\
&= \eta\left(\int_0^\infty p(y/x)\ln\left[\frac{p(y/x)}{P(p(y/u))}\right]dy\right) - \left(\int_0^\infty P(p(y/x))\left[\frac{\eta(p(y/u))}{P(p(y/u))}\right]dy\right) \\
&= \eta\left(\int_0^\infty p(y/x)\ln\left[\frac{p(y/x)}{P(p(y/u))}\right]dy\right) - \left(\int_0^\infty \eta(p(y/u))dy\right) \\
&= \eta\left(\int_0^\infty p(y/x)\ln\left[\frac{p(y/x)}{P(p(y/u))}\right]dy - 1\right)
\end{aligned}$$

The constraints we have are clearly Gateaux differentiable, so Condition 3 is also satisfied. The differentials are

$$\partial[(P+\lambda\eta)(1_{[\alpha,\alpha+\beta]})]/\partial\lambda_{|\lambda=0} = \eta(1_{[\alpha,\alpha+\beta]}),$$

and

$$\partial[(P+\lambda\eta)(x^2)]/\partial\lambda_{|\lambda=0} = \eta(x^2).$$

Checking whether Condition 4 is satisfied or not is a very complex matter due to the diffi-

culties of finding an appropriate topology in the space Z. We assume this condition to be also satisfied, so we can apply the theorem.

Since $P(1)$,and $P(x^2)$ take all their values in the vector space R, the Lagrange multipliers to be associated with constraints $P(1)=1$, and $P(x^2)-a \leq 0$, are also real. These multipliers will be denoted λ_1, and λ_2 respectively.

On the other hand, since $P(1_{[\alpha,\alpha+\beta]})$ is a function of α and β, the Lagrange multiplier to be associated with the constraint $P(1_{[\alpha,\alpha+\beta]}) \geq 0 \ \forall\alpha\geq 0$ and $\forall\beta\geq 0$, is also a function of α and β, denoted $\gamma(\alpha,\beta)$.

Since distributions are linear, the generalized Kuhn-Tucker theorem states that

$$-\int_0^\infty p(y/x)\ln\left[\frac{p(y/x)}{p(y)}\right]dy + 1 + \lambda_1 1 + \lambda_2 x^2 - \iint \gamma(\alpha,\beta)\,1_{[\alpha,\alpha+\beta]} = 0 \quad \forall x, \tag{A.1}$$

and the multipliers should satisfy

$$\lambda_1(P(1)-1) + \lambda_2(P(x^2)-a) - \iint \gamma(\alpha,\beta)P(1_{[\alpha,\alpha+\beta]}) = 0.$$

Each term of the above expression is negative (all the multipliers are greater or equal to zero). Therefore, each one of them is null. Let's look what implications this result has on $\gamma(\alpha,\beta)$.

$$\iint \gamma(\alpha,\beta)P(1_{[\alpha,\alpha+\beta]})d\alpha d\beta = 0 \Leftrightarrow P\left(\iint \gamma(\alpha,\beta)\,1_{[\alpha,\alpha+\beta]}d\alpha d\beta\right) = 0. \tag{A.2}$$

Since $\gamma(\alpha,\beta)$ is non-negative, $\iint \gamma(\alpha,\beta)\,1_{[\alpha,\alpha+\beta]}d\alpha d\beta$ is a non-negative function of x.

Assume that we can separate the probability distribution P into two terms: $P = \sum_i p_i\delta_{x_i} + Tf$, where Tf is the distribution associated to a function f, and δ_x the usual Dirac distribution at x. The use of the symbol Σ is justified by the fact that we cannot possibly have more than a *countable* number of impulses, as it is argued in [13]. Note that the constraints imply that the p_i's and $f(x)$ should be non-negative.

Having made this assumption, equation (A.2) implies that $\iint \gamma(\alpha,\beta)\,1_{[\alpha,\alpha+\beta]}d\alpha d\beta = 0$ wherever $f(x)$ is positive, or $x = x_i$ (assuming $p_i>0\ \forall i$).

Equation (A.1) can now be written in the following form:

$$-\int_0^{\infty} p(y/x)\ln\left[\frac{p(y/x)}{p(y)}\right]dy + 1 + \lambda_1 1 + \lambda_2 x^2 \geq 0 \quad \forall x\,,$$

with equality for $x = x_i$ or such that $f(x)$ is positive.

Now if we let C be such that $1+\lambda_1=C-\lambda_2 a$, we obtain

$$-\int_0^{\infty} p(y/x)\ln\left[\frac{p(y/x)}{p(y)}\right]dy + C + \lambda_2(x^2 - a) \geq 0 \quad \forall x\,. \tag{A.3}$$

We still need to prove that C is the capacity of the channel. Let's take the expectation of equation (A.3) with respect to the optimal probability density, we obtain $C=I(X,Y)$. Thus, C is indeed the channel capacity.

Appendix B

The Accumulation Point

Assume that $p^*(s)$ is positive over an infinite set of points $S_S \subset \left[\frac{1}{1+A^2}, 1\right] \subset (0, 1]$. Let's consider next the closure S of S_S. S is a closed and bounded set in R, and thus it is a compact set. Using the Bolzano-Weierstrass theorem on the compact S, any infinite sequence of distinct points of $S_S \subset S$ has a point of accumulation in $S \subset \left[\frac{1}{1+A^2}, 1\right] \subset (0, 1]$.

Therefore, S_S has an accumulation point in the interval (0,1].

Appendix C

Proof of Theorem 1

Theorem 1: Let $p(y)$ be a probability density function with mean m. If $f(y)$ is a monotonically decreasing function then $\int (y-m)p(y)f(y)dy < 0$.

Corollary 1: For a monotonically increasing function then clearly we have $\int (y-m)p(y)f(y)dy > 0$.

Proof of Theorem 1:

Let's write the integral as a sum of two terms

$$\int_{-\infty}^{\infty} (y-m)p(y)f(y)dy = \int_{-\infty}^{m} (y-m)p(y)f(y)dy + \int_{m}^{\infty} (y-m)p(y)f(y)dy .$$

For $y<m$, since $f(y)$ is decreasing, $f(y)>f(m)$ and therefore $(y\text{-}m)p(y)f(y) < (y\text{-}m)p(y)f(m)$. Hence,

$$\int_{-\infty}^{m} (y-m)p(y)f(y)dy < f(m)\int_{-\infty}^{m} (y-m)p(y)dy .$$

On the other hand, for $y>m$ we have $f(y)<f(m)$ and since $(y\text{-}m)$ is positive $(y\text{-}m)p(y)f(y) > (y\text{-}m)p(y)f(m)$. Therefore,

$$\int_{m}^{\infty} (y-m)p(y)f(y)dy < f(m)\int_{m}^{\infty} (y-m)p(y)dy .$$

Combining these inequalities with the fact that m is the mean of Y, we conclude

$$\int_{-\infty}^{\infty} (y-m)p(y)f(y)dy < f(m)\int_{-\infty}^{\infty} (y-m)p(y)dy = 0 .$$

Appendix D

Condition for an Additional Impulse

A necessary condition for x to be the optimal mapping is clearly

$$\frac{\partial}{\partial \varepsilon} J(x+\varepsilon\eta)|_{\varepsilon=0} = 0 \text{ for all admissible perturbation functions } \eta(t), \tag{D.1}$$

and

$$\frac{\partial^2}{\partial \varepsilon^2} J(x+\varepsilon\eta)|_{\varepsilon=0} \le 0 . \tag{D.2}$$

A necessary condition for bifurcation is to have exact equality in (D.2) for some perturbation η (the question of higher derivatives is disregarded as only a necessary condition is of interest).

After straightforward differentiation, we find that (D.1) is equivalent to

$$\int_0^\infty \frac{\partial}{\partial x} p(y/x) \ln\left[\frac{p(y/x)}{p(y)}\right] dy - 2\rho(x) = 0 ,$$

and the condition for equality in (D.2) is

$$\int_{[0,1]} \left[\int_0^\infty \frac{\partial^2}{\partial x^2} p(y/x) \ln\left[\frac{p(y/x)}{p(y)}\right] dy + \int_0^\infty \left(\frac{\partial}{\partial x} p(y/x)\right)^2 \left[\frac{1}{p(y/x)}\right] dy - 2\rho \right] \eta^2 d\mu$$

$$- \int_0^\infty \left(\int_{[0,1]} \frac{\partial}{\partial x} p(y/x) \eta \, d\mu \right)^2 \cdot \frac{1}{\int_{[0,1]} p(y/x) d\mu} dy = 0 \tag{D.3}$$

Following similar steps to what has been done in Rose's paper [12], we are going to prove that the sum in (D.3) is negative for all η *if and only if* the first term is.

The "if" part is trivial since the second term is obviously nonpositive. To prove the "only if" part we use the fact that the input is discrete. For the first term to be nonnegative, there must be at least one point of support x_0 of nonzero mass such that

$$\int_0^\infty \frac{\partial^2}{\partial x^2} p(y/x_0) \ln\left[\frac{p(y/x_0)}{p(y)}\right] dy + \int_0^\infty \left(\frac{\partial}{\partial x} p(y/x_0)\right)^2 \left[\frac{1}{p(y/x_0)}\right] dy - 2\rho \ge 0 .$$

The mass of x_0 is the measure of the subset $I_0 \in [0,1]$ that is mapped to x_0. Let's choose $\eta(t)$ such that $\eta(t)=0$, $\forall t \notin I_0$, to ensure that the first term is nonnegative. The second term is then

$$-\int_0^\infty \left[\frac{\partial}{\partial x} p(y/x_0) \int_{I_0} \eta(t) d\mu(t)\right]^2 \cdot \frac{1}{\int_{[0,1]} p(y/x) d\mu} dy .$$

We have not yet specified the function $\eta(t)$ at $t \in I_0$, which we can always define so that

$$\int_{I_0} \eta(t) d\mu(t) = 0 .$$

Hence, whenever the first term is not negative, we can choose a perturbation function such that the second term vanishes. The conclusion is therefore that we have strict inequality in (D.2) for all $\eta(t)$ if and only if the first term in (D.3) is negative.

Consequently, the condition for an impulse to be added (equality in equation (D.2)) can be restated as follows: there exists some point of support x_0 for which we have

$$\int_0^\infty \frac{\partial^2}{\partial x^2} p(y/x_0) \ln\left[\frac{p(y/x_0)}{p(y)}\right] dy + \int_0^\infty \left(\frac{\partial}{\partial x} p(y/x_0)\right)^2 \left[\frac{1}{p(y/x_0)}\right] dy - 2\rho = 0 .$$

References

[1] John S. Richters "Communication Over Fading Dispersive Channels" Research Laboratory of Electronics, Technical Report 464. Nov 30, 1967.

[2] Robert G. Gallager "Information Theory and Reliable Communication" John Wiley & Sons Inc., 1968.

[3] Thomas M. Cover, Joy A. Thomas "Elements of Information Theory" John Wiley & Sons Inc., 1991.

[4] Robert S. Kennedy "Fading Dispersive Communication Channels" John Wiley & Sons Inc., 1969.

[5] G. Saporta "Probabilités et Statistique" Cours de l'École Centrale Paris, 1992-1993.

[6] J.G. Smith, "The Information Capacity of Amplitude and Variance-Constrained Scalar Gaussian Channels", Inform. Contr., vol. 18, pp. 203-219, 1971.

[7] S. Shamai and I. Bar-David, "The Capacity of Average and Peak-Power-Limited Quadrature Gaussian Channels", IEEE Trans. Inform. Theory, vol. 41, no. 4, pp. 1060-1071, July 1995.

[8] C. Lamoureux, "Analyse Mathématique et Numérique" Cours de l'École Centrale Paris, 1992-1993.

[9] Herb Silverman, "Complex Variables" Houghton Mifflin Company, 1975.

[10] David G. Luenberger, "Optimization by Vector Space Methods" John Wiley & Sons Inc., 1969.

[11] D. Verwaerde, "Analyse Numérique et Modélisation" Cours de l'École Centrale Paris, 1992-1993.

[12] Kenneth Rose, "A Mapping Approach to Rate-Distortion Computation and Analysis", IEEE Trans. Inform. Theory, vol. 40, no. 6, pp. 1939-1952, November 1994.

[13] Kai Lai Chung, "A Course in Probability Theory" Second Edition, Academic Press Inc., 1974.